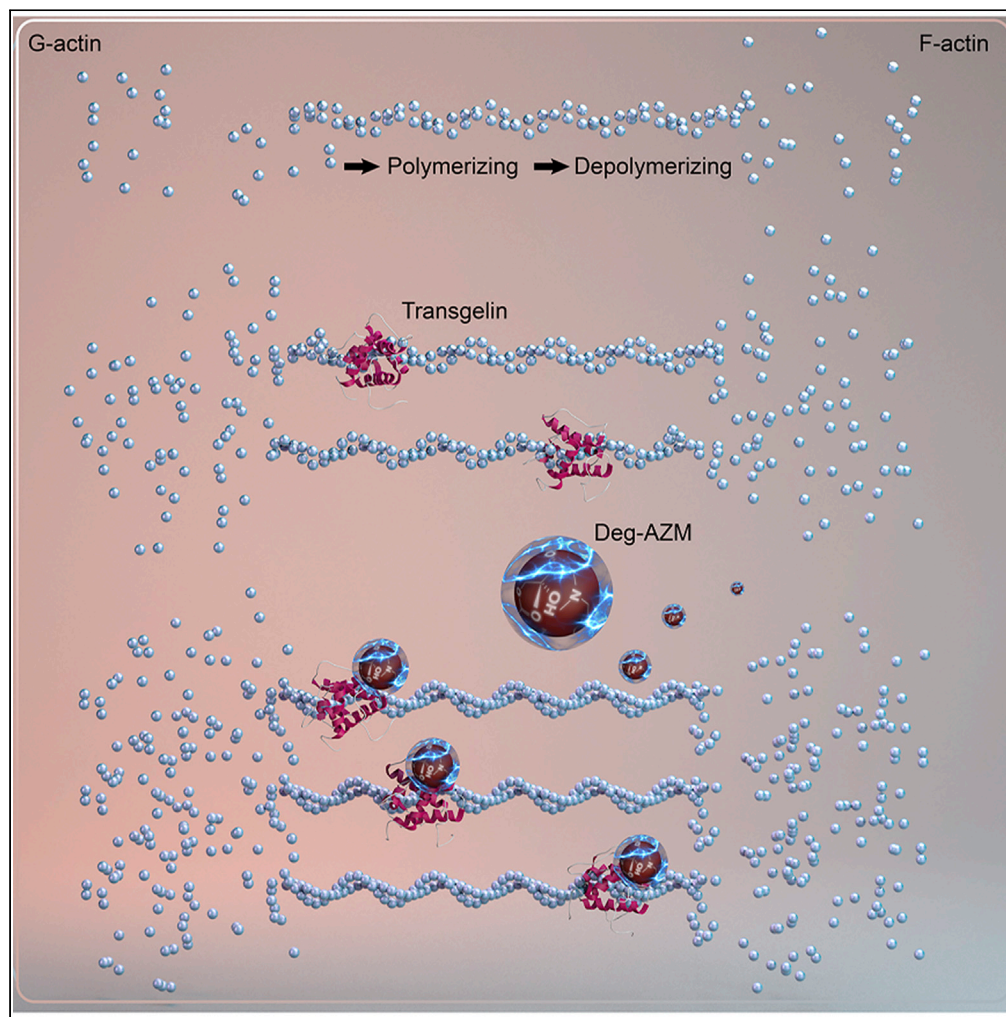CellPress
OPEN ACCESS

Article

Deglycosylated Azithromycin Targets Transgelin to Enhance Intestinal Smooth Muscle Function

Weilong Zhong, Bo Sun, Hao Ruan, ..., Cheng Yang, Tao Sun, Honggang Zhou

mwang02@tmu.edu.cn (B.W.)
cheng.yang@nankai.edu.cn (C.Y.)
sunrockmia@hotmail.com (T.S.)
honggang.zhou@nankai.edu. cn (H.Z.)

HIGHLIGHTS

AZM to promote bowel motility was attributed to the metabolism of Deg-AZM

Transgelin was identified and validated as the direct target of Deg-AZM

Deg-AZM affected dynamics of the actin cytoskeleton by stabilizing actin filaments

Transgelin may be a potential therapeutic target for the constipation

Article

Deglycosylated Azithromycin Targets Transgelin to Enhance Intestinal Smooth Muscle Function

Weilong Zhong,[2,3,6] Bo Sun,[3,6] Hao Ruan,[1,6] Guang Yang,[1,6] Baoxin Qian,[4,6] Hailong Cao,[2,3,6] Lingfei He,[1] Yunjing Fan,[1] Arthur G. Roberts,[5] Xiang Liu,[2] Xuejiao Hu,[1] Yuan Liang,[1] Qing Ye,[4] Tingting Yin,[1] Bangmao Wang,[2,*] Cheng Yang,[1,3,*] Tao Sun,[1,3,7,*] and Honggang Zhou[1,3,*]

SUMMARY

Azithromycin (AZM) has been widely used as an antibacterial drug for many years. It has also been used to treat delayed gastric emptying. However, it exerts several side effects. We found that deglycosylated AZM (Deg-AZM or CP0119), an AZM metabolite, is a positively strong intestinal agonist that may result in the intestinal mobility experienced by patients after AZM administration. We confirmed that Deg-AZM can function strongly on intestinal peristalsis and identified transgelin as its potential molecular target. Furthermore, our pharmacological studies showed that the binding of Deg-AZM to transgelin enhanced the contractility of intestinal smooth muscle cells by facilitating the assembly of actin filaments into tight bundles and stress fibers. Specifically, Deg-AZM promoted intestinal peristaltic activity in wild-type mice but not in transgelin ($-/-$) mice. Moreover, Deg-AZM did not exert antibacterial activity and did not disrupt intestinal flora. Thus, Deg-AZM may become a potential drug for slow-transit constipation treatment.

INTRODUCTION

Prolonged delay in stool transit through the colon is a typical characteristic of slow-transit constipation (Sharma and Rao, 2017), which results from numerous reasons. Increasing colonic smooth muscle contraction can effectively treat this symptom. Current therapeutic drugs for constipation are mainly guanylate cyclase and 5-hydroxytryptamine (5-HT, serotonin) receptor agonist (Kim et al., 2017; Malagelada et al., 2017; Shah et al., 2018). Some 5-HT$_4$ agonists, such as cisapride and tegaserod, can be used to treat constipation, constipation-predominant irritable bowel syndrome, functional dyspepsia, or gastroparesis (Deruyttere et al., 1987; Johanson, 2004; Johanson et al., 2004; Mansour et al., 2012; Ueno et al., 2010). However, these drugs may cause some side effects, including nausea, headache, and prolonged QT interval. Cisapride was even withdrawn from the market because it exerts cardiovascular side effects, which stem from its poor selectivity over human potassium channels (Corvaglia et al., 2004; Drolet et al., 1998; Satoh et al., 2000; Wang et al., 2001). In addition, long-term use of agonists may lead to drug resistance (Shen, 2009; Van Outryve et al., 1993). Some traditional natural medicines, such as rhubarb, senna leaves, and aloe, used to treat constipation contain diarrheal ingredients. Clinical practice has confirmed that the long-term use of rhubarb, senna leaves, and aloe may result in colorectal melanosis, which may induce colorectal cancer development (Kav and Bayraktar, 2010).

The antibiotic drugs erythromycin (EM) and azithromycin (AZM) have gastrointestinal stimulation effects given that they are motilin-receptor agonists (Broad and Sanger, 2013; Chini et al., 2012; Depoortere et al., 1990; Moshiree et al., 2010; Sanger and Furness, 2016). Erythromycin and azithromycin can stimulate gastric and intestinal tissues, respectively (Chini et al., 2012). The side effects of both drugs vary widely among different populations. AZM, which is a macrolide compound, can be used to treat gastrointestinal dysmotility (Potter and Snider, 2013). However, the long-term use of antibiotics may exacerbate the spread of antibiotic-resistant pathogens.

In this study, we found that deglycosylated azithromycin (Deg-AZM), an AZM metabolite, is a positively strong intestinal agonist that induces intestinal mobility, which is a frequently observed side effect of AZM. We also determined that Deg-ZAM binds to transgelin, a structural protein that binds to actin

[1]State Key Laboratory of Medicinal Chemical Biology and College of Pharmacy, Nankai University, Tianjin 300350, China

[2]Department of Gastroenterology and Hepatology, Tianjin Medical University General Hospital, Tianjin Institute of Digestive Disease, Tianjin 300052, China

[3]Tianjin Key Laboratory of Early Druggability Evaluation of Innovative Drugs and Tianjin Key Laboratory of Molecular Drug Research, Tianjin International Joint Academy of Biomedicine, Tianjin 300450, China

[4]Department of Gastroenterology and Hepatology, Tianjin Key Laboratory of Artificial Cells, Tianjin Institute of Hepatobiliary Disease, Tianjin Third Central Hospital, Tianjin 300041, China

[5]Department of Pharmaceutical and Biomedical Sciences, University of Georgia, Athens, GA 30602, USA

[6]These authors contributed equally

[7]Lead Contact

*Correspondence:
mwang02@tmu.edu.cn (B.W.),
cheng.yang@nankai.edu.cn (C.Y.),
sunrockmia@hotmail.com (T.S.),
honggang.zhou@nankai.edu.cn (H.Z.)
https://doi.org/10.1016/j.isci.2020.101464

(Elsafadi et al., 2016; Lee et al., 2010; Thompson et al., 2012; Zhou et al., 2016). Transgelin contains a c-terminal calponin-like module (CLIK[23]) and an upstream region of positively charged amino acids for binding to actin. Transgelin is mainly distributed in smooth muscle tissue. Transgelin participates in the organization of the actin cytoskeleton and facilitates the assembly of actin filaments into bundles in smooth muscle cells (SMCs) (Elsafadi et al., 2016; Lees-Miller et al., 1987a, 1987b) to form additional and strong contractile structures that provide contraction forces to intestinal SMCs. Acting together with myosin (a molecular motor protein), actin hydrolyzes the phosphate group at the end of ATP and also hydrolyzes GTP, CTP, etc. converting chemical energy into mechanical energy, resulting in various forms of motion that increase the contraction of smooth muscle cells. As an actin-binding protein, transgelin can promote G-actin to F-actin aggregation. Reduce treadmilling, increase F/G-actin ratio in intestinal smooth muscle cells, increase the length and strength of fiber bundles, and thereby increase the contraction ability of smooth muscle cells.

RESULTS

Deg-AZM Can Strengthen Intestinal Peristalsis

AZM induces inconsistent intestinal peristaltic effects (Chini et al., 2012; Moshiree et al., 2010). The same patient may exhibit different responses at different time points after AZM treatment. Moreover, AZM has poor acid resistance, and only few AZM molecules can reach the colon. AZM metabolites in the intestinal microenvironment and produced by intestinal bacteria may induce intestinal peristalsis. Our analysis of the *in vivo* metabolites of AZM indicates that Deg-AZM is an *in vivo* AZM metabolite that is associated with AZM-induced bowel movement.

We recruited 38 healthy volunteers. They consented to receive AZM orally in accordance with a doctor's instructions. The volunteers who demonstrated gastrointestinal tract reaction within 24 h were grouped into the positive group, whereas those who failed to show reactions were categorized as the negative group (Figure 1A). Then, the fecal samples of healthy volunteers were collected and subjected to mass spectrometry (Figures 1B–1C). The results for volunteers with Deg-AZM-containing feces and those with gastrointestinal reactions were subjected to statistical analysis (Figure 1D). A significant correlation existed between the generation of Deg-AZM and intestinal peristalsis. The χ^2 of the association between Deg-AZM and intestinal peristalsis were 14.198 and the p values less than 0.001.

We collected fecal samples from mice, rats, rabbits, dogs, and humans. We incubated fecal samples separately with AZM to verify if intestinal bacteria produced Deg-AZM from AZM. We further analyzed fecal samples through mass spectrometry (Figure 1E). Deg-AZM was indeed detected in feces incubated with AZM solution (Figure 1F). The gradual increment in Deg-AZM concentration with the prolongation of incubation time (Figure 1G) indicates that intestinal bacteria can form Deg-AZM by deglycosylating AZM.

Bifidobacterium Can Deglycosylate AZM to Produce Deg-AZM

Four bacteria, *Escherichia coli*, *Lactobacillus*, *Bifidobacterium*, and *Enterococcus,* were used to identify which intestinal bacteria can deglycosylate AZM and produce Deg-AZM. The *Bifidobacterium* was the only bacteria of those examined that produced significant amounts of Deg-AZM (Figure 2A). Deg-AZM concentration also increased as incubation time was increased (Figure 2B).

We recruited 36 patients with constipation to further verify our results. We divided the patients into two groups. Patients in one group ingested AZM (3 days) alone and another ingested AZM for 3 days after taking bifidobacteria for 3 days (Figure 2C). The subjective and macroscopic efficiency of the two treatments were 33.3% and 55.5%, respectively (Figure 2D). The results for the two treatments were subjected to statistical analysis. The correlation between adoptive therapy and promoting intestinal peristalsis was positive (Figure 2E). This result also suggests that the intestinal side effects of AZM may be potentially induced by Deg-AZM.

Deg-AZM Can Strengthen Intestinal Peristalsis in Mice, Rabbits, Dogs, and Monkey Models

We synthesized three compounds to study if Deg-AZM can promote bowel movement (Figure 3A). The detailed synthesis steps and characterization results are shown in Figures S1–S7. Animal experiments were performed in accordance with the procedure shown in Figure 3B. All animals are on a regular diet (Table S1). Carbon propelling was conducted to evaluate the changes induced in intestinal peristalsis by all
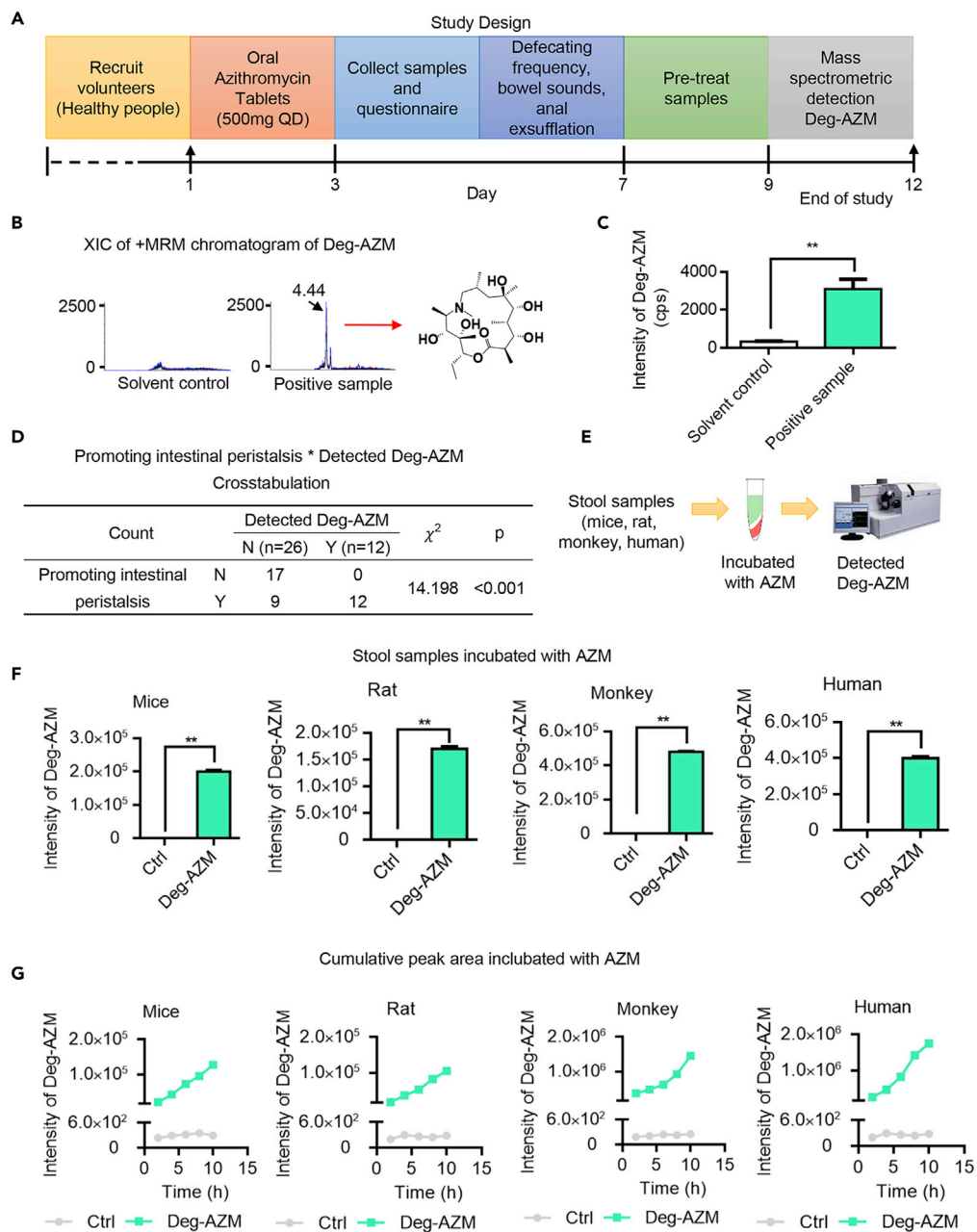
Figure 1. Deg-AZM, an AZM Metabolite, Can Be Produced by Intestinal Microflora

(A) Process of the *in vivo* clinical experimental performed to verify that Deg-AZM is a metabolite of AZM.

(B) Fecal samples were determined by mass spectrometry after administration of azithromycin.

(C) Statistical results of Deg-AZM content in different groups. Mass spectrometry revealed that Deg-AZM was present in human stool samples after oral AZM administration. XIC (Extraction ion Ion Flow Chromatography), MRM (multiple reaction monitoring). $**p < 0.01$, Student's t test.

(D) Correlation analysis between promoting intestinal peristalsis and detection of Deg-AZM. χ^2 test showed that Deg-AZM and increased intestinal peristalsis are positively correlated. Chi-square test.

(E) Schematic for the detection of Deg-AZM in fecal samples through mass spectrometry.

(F) Analysis of Deg-AZM after incubation of azithromycin and fecal samples. Deg-AZM was present in stool samples from different animals and incubated with AZM. $**p < 0.01$, Student's t test.

(G) Deg-AZM concentration in the stool samples of different animals increased with time after oral AZM administration. Error bars represent mean $\pm$ SD, $*p < 0.05$, $**p < 0.01$.
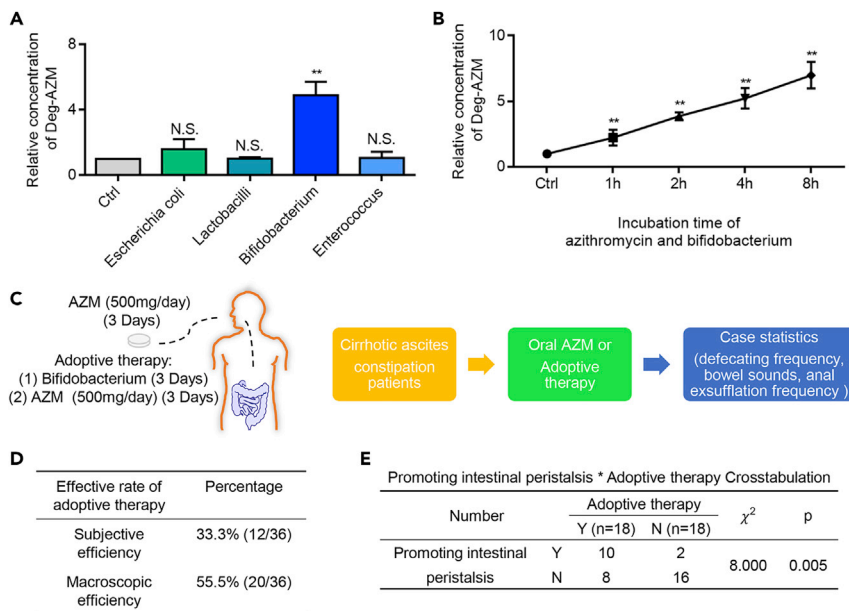
Figure 2. Bifidobacteria Can Degrade AZM to Produce Deg-AZM

(A) The content of Deg-AZM was detected by mass spectrometry after incubation of azithromycin and intestinal bacteria. Deg-AZM concentration after AZM was incubated with different bacteria was quantified through mass spectrometry. **$p < 0.01$, one-way ANOVA.

(B) Deg-AZM concentration increased with the prolongation of bifidobacteria and AZM incubation. **$p < 0.01$, one-way ANOVA.

(C) Schematic of the treatment received by patients with constipation.

(D) Effective rates of AZM alone and adoptive therapy method for patients with constipation.

(E) Correlation analysis between promoting intestinal peristalsis and adoptive therapy. χ^2 test revealed a positive correlation between intestinal peristalsis and AZM. $p = 0.005$, Chi-square test. Error bars represent mean $\pm$ SD, *$p < 0.05$, **$p < 0.01$.

compounds. Prucalopride, a 5-HT$_4$ receptor agonist, was used as the positive control. We tested the induction of intestinal peristalsis by orally administered AZM, AZM-1, Deg-AZM, and prucalopride in atropine- and sucralfate-induced mouse constipation models. We found that intestinal peristalsis significantly increased in the Deg-AZM group relative to that in the model group. Moreover, the carbon propulsion capacity of Deg-AZM was similar to the positive control prucalopride within the error (Figures 3C and 3D). Deg-AZM exerted its effect in a dose-dependent manner. The rate of carbon propelling in the AZM-1 group negligibly differed from that in the model group. In testing the effect of Deg-AZM on intestinal peristalsis shown in the supplementary experiment (Figure S8), results showed that the weight of feces, number of feces, and animal food intake after drug administration increased in dose and response relationship, which indicates the increasing smooth muscle contractility by Deg-AZM may be the main source of its efficacy. Deg-AZM also induced intestinal peristalsis in other animals, such as guinea pigs, rabbits, dogs, and monkeys (Figures 3E–3F). Thus, Deg-AZM can promote intestinal peristalsis in different animal models.

Deg-AZM Can Selectively Stimulate Intestinal Smooth Muscles but Not Gastric Smooth Muscles

AZM and EM enhance gastrointestinal peristalsis by binding to motilin receptors (MTLRs) (Broad and Sanger, 2013; Chini et al., 2012; Depoortere et al., 1990; Moshiree et al., 2010; Sanger and Furness, 2016). We further evaluated whether Deg-AZM has the same activity on motilin receptors by performing a calcium flow experiment. We employed an HEK-293 cell line transfected with motilin-receptor vectors (Figure S9). Deg-AZM lacked motilin-receptor agonist activity (Figure 4A). This result implies that Deg-AZM may have a new target. We prepared and tested Deg-AZM, AZM, and EM molecule probes with the ability to enhance intestinal peristaltic activity to determine the potential target and tissue distribution of Deg-AZM (Figures 4B–4C and S10). Different gastrointestinal sections were stained through click chemistry after treatment with different agents. Deg-AZM was mainly found in the intestine, and EM mainly
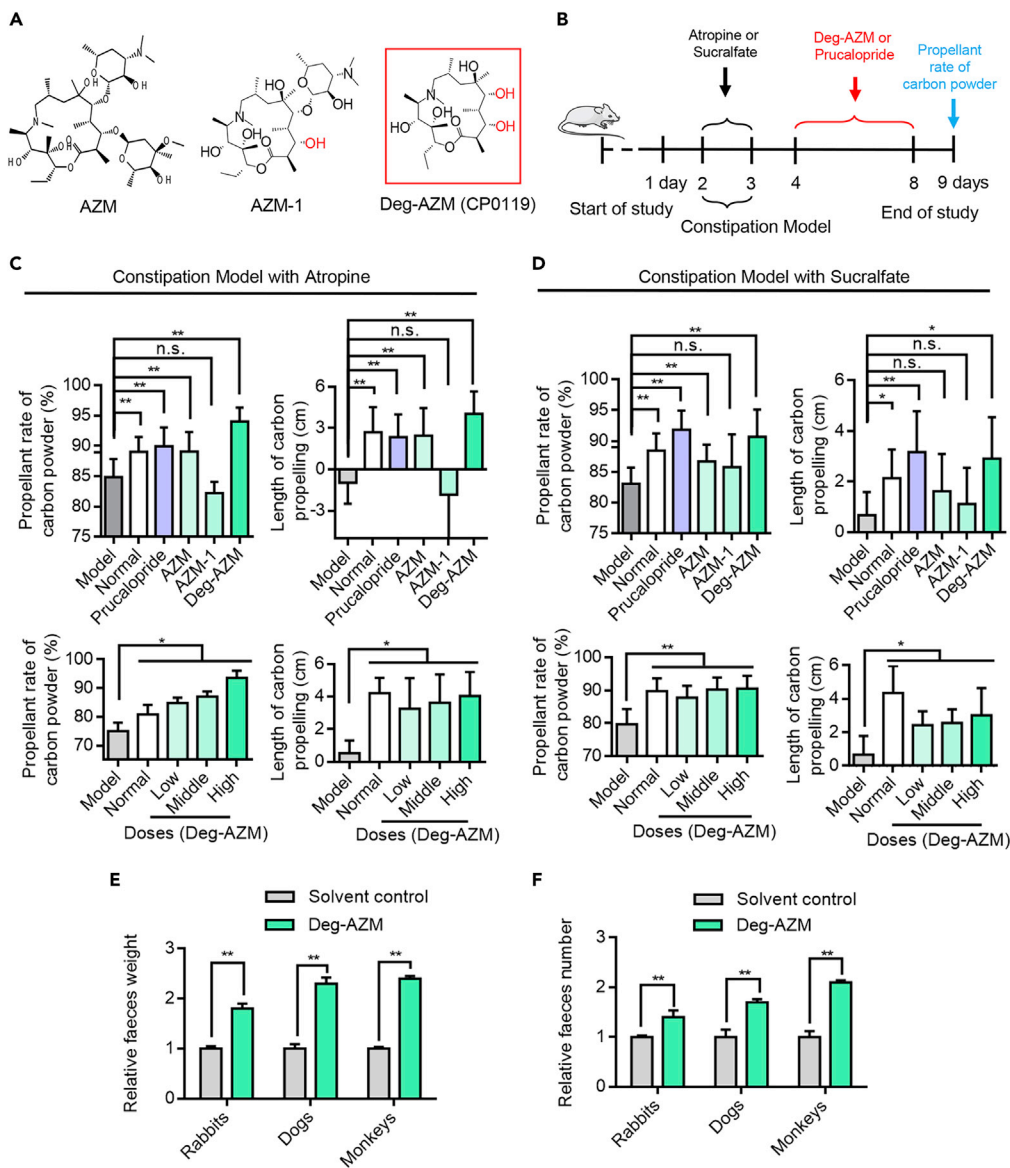
Figure 3. Deg-AZM Significantly Increases Gastrointestinal Motility

(A) Structures of AZM, AZM-1, and Deg-AZM.

(B) Model method of constipation model and schematic diagram of Deg-AZM therapy experiment.

(C) Propellant rate and propelling distance of carbon powder in atropine-induced mouse constipation models treated with different compounds. Deg-AZM significantly increased the weight of defecation and the number of defecation granules and was dose dependent. **p < 0.01, *p < 0.05, one-way ANOVA.

(D) Propellant rate of carbon powder and carbon propelling distance of Deg-AZM in the sucralfate-induced mouse constipation model. **p < 0.01, *p < 0.05, one-way ANOVA.

(E) Prokinetics effect of Deg-AZM on the intestinal tracts of rabbits, dogs, and monkeys. Deg-AZM significantly increased the faeces weight of bowel movements in animals. **p < 0.01, Student's t test.

(F) Deg-AZM significantly increased the faeces number of bowel movements in animals. **p < 0.01, Student's t test. Each bar represents the mean ± SD for different animal measurements.

localized in the stomach. AZM was observed in the stomach and intestine (Figure 4D). We collected and stained tissue sections from mice fed with probes. The *in vivo* results for different time points were similar to the *in vitro* results (Figure 4E). To verify the tissue selectivity of EM, AZM, and Deg-AZM, we performed *in vitro* muscle tension studies. Results showed that Deg-AZM enhanced the contraction amplitude and frequency of intestinal smooth muscle cells, and EM enhanced those of gastric smooth muscle. AZM
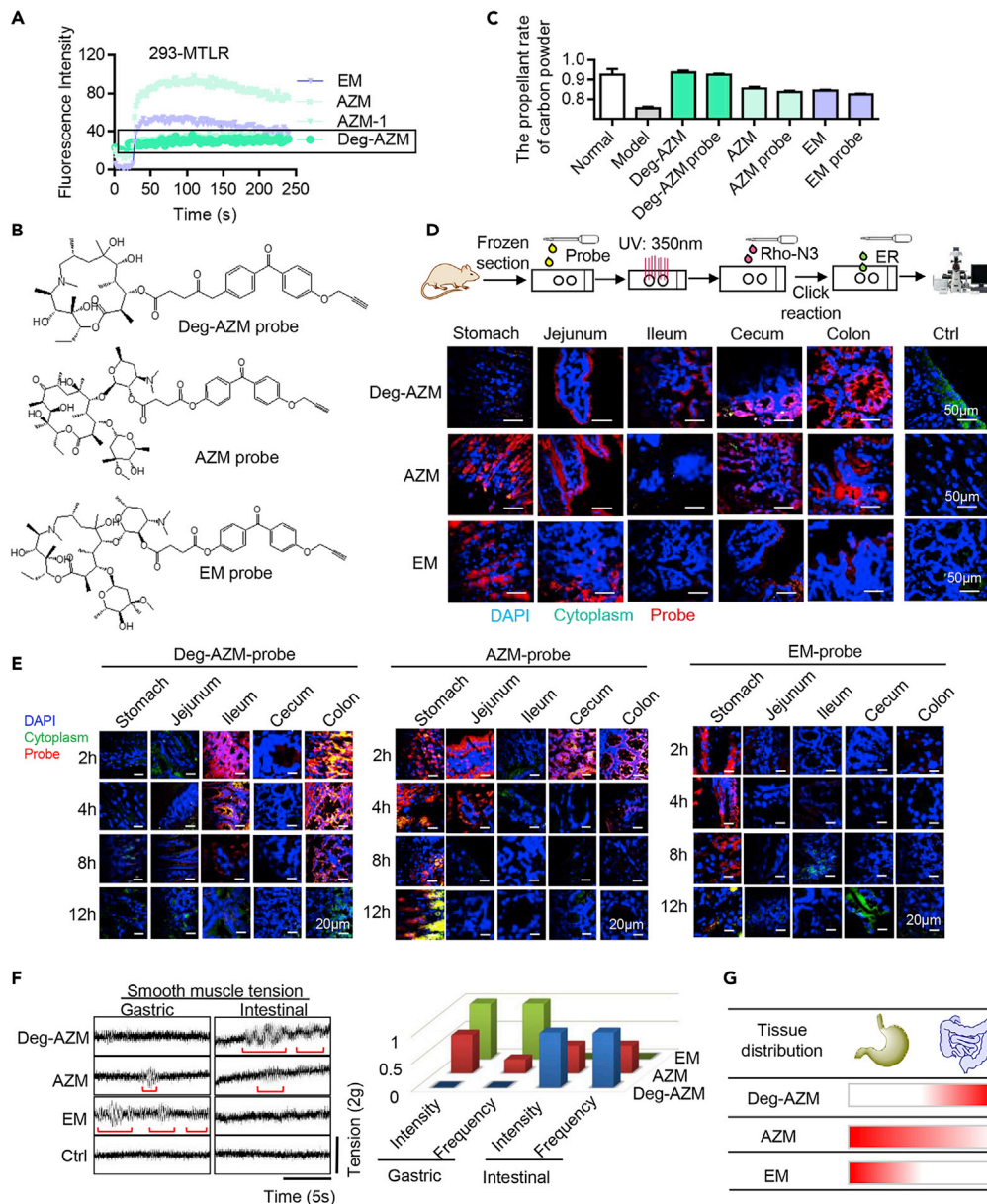
Figure 4. Deg-AZM Selectively Activates Intestinal Tissues

(A) Calcium flow test results for the 293 cell line overexpressing motilin receptor treated with AZM, EM, Deg-AZM, and other derivatives. Deg-AZM had no excitatory activity on the motilin receptor and did not cause changes in the calcium flow signal of the motilin receptor.

(B) Structure of Deg-AZM, AZM, and EM probes. Probe with diphenyl ketone as linkers.

(C) Propellant rate of carbon powder by AZM, EM, and Deg-AZM probes. The experimental results showed that the modification of ligands did not affect the bioactivity of small molecules and could be used as subsequent tissue staining.

(D) Different images of tissue samples from mice fed with AZM, EM, and Deg-AZM probes. The red fluorescence is small-molecule probe fluorescence. The higher the fluorescence intensity, the higher the concentration of small molecules in tissues.

(E) Different mouse tissue images obtained at different time points after feeding with AZM, EM, and Deg-AZM probes separately.

(F) Muscle tension of different tissues tested by a multiple physiological recorder after AZM, EM, and Deg-AZM treatment. The tissues used were colon tissues of mice. Deg-AZM increases the amplitude and frequency of colon contractions. The abscissa indicated time, and the ordinate indicated contraction amplitude of colon.

(G) Schematic of the tissue locations of Deg-AZM, AZM, and EM. Deg-AZM selectively stimulated intestinal tissues.
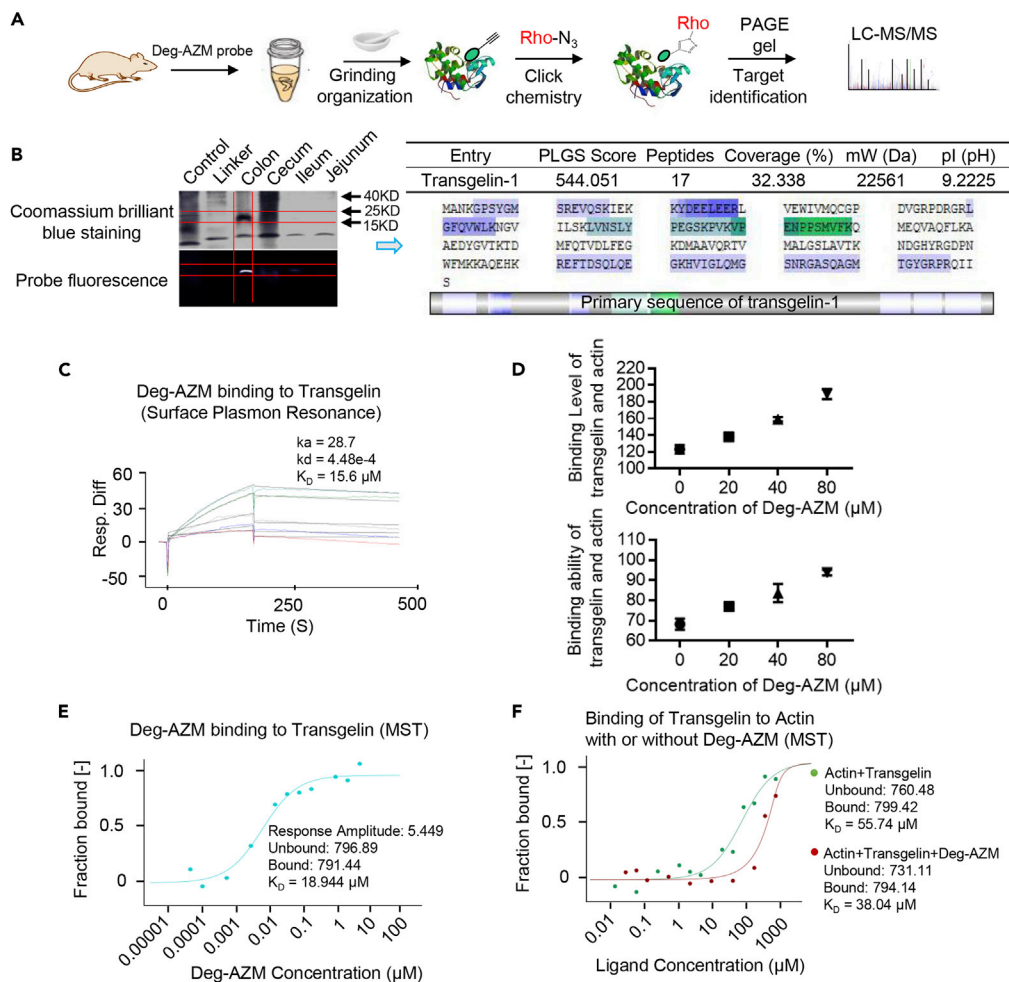
Figure 5. Deg-AZM Targets Transgelin to Promote the Contraction and Energy Utilization of Intestinal SMCs

(A) Schematic of target identification in mouse tissues with the Deg-AZM probe.

(B) Results of Deg-AZM probe target fishing and mass spectrometry identification. Transgelin-1 was identified as a potential Deg-AZM target.

(C) Validation results of Deg-AZM and target protein. Biacore result for Deg-AZM binding to transgelin. The equilibrium dissociation constant (Kd) between Deg-AZM and transgelin was 15.6 μM as measured through the Biacore assay.

(D) Binding level and stability between transgelin and actin increased with the addition of Deg-AZM.

(E) MST result for the binding of Deg-AZM to transgelin. The Kd value obtained through MST assay was 18.944 μM.

(F) MST assay showed that Deg-AZM increased transgelin binding to actin protein.

enhanced the amplitude and frequency of smooth muscle contraction both in the stomach and intestine tissues (Figure 4F). These results suggest the Deg-AZM selective activation of intestinal tissue (Figure 4G). The target of Deg-AZM should be studied and identified from intestinal muscle cells.

Deg-AZM Can Bind to Transgelin to Increase the Contractile Capacity of Intestinal SMCs

By performing Deg-AZM probe fishing and mass spectrometry detection, we identified transgelin-1 as a potential target of Deg-AZM in colon tissue (Figures 5A and 5B and Table S2). Transgelin was significantly expressed in colon tissue. We conducted Biacore analysis, mass spectrometry identification, and micro-scale thermophoresis (MST) to further verify that Deg-AZM binds to transgelin (Figures 5C, 5D, 5E, and S11). The results of these analyses support that Deg-AZM directly bound to transgelin in a concentration-dependent manner with the micromolar binding affinity of Kd = 15.6 μM. MST results showed that Deg-AZM increased the interaction of transgelin and actin, and the dissociation constant (Kd value of transgelin to actin) increased from 55.74 μM to 38.04 μM (Figure 5F).
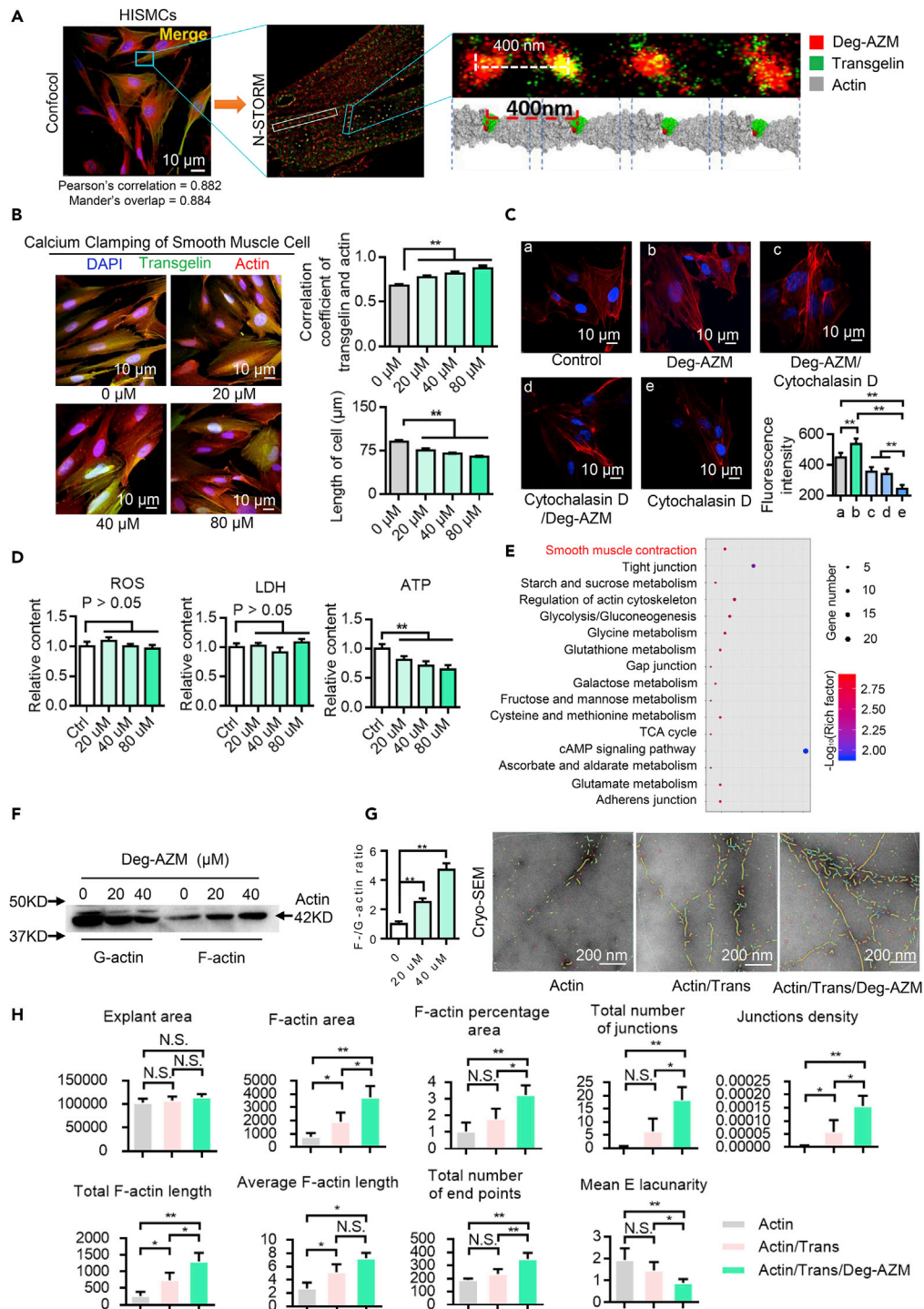
Figure 6. Deg-AZM Promotes Actin Polymerization to F-actin

(A) Deg-AZM colocalized with transgelin in intestinal SMCs. The Pearson's correlation of Deg-AZM and transgelin is 0.882 and Mander's overlap is 0.884.

(B) HISMCs were treated with different Deg-AZM concentrations for 24 h. Then, cell length and the correlation between the locations of transgelin and actin were quantified. **$p < 0.01$, one-way ANOVA.

(C) After different treatments, F-actin of intestinal smooth muscle cells was detected. Cytochalasin D (actin inhibitor, 0.5 μM for 24 h) can reduce F-actin bundling, but its effect was weakened by Deg-AZM. **$p < 0.01$, one-way ANOVA.

Figure 6. Continued

(D) ROS, LDH, and ATP concentrations of HISMCs after treatment with different Deg-AZM concentrations. **p < 0.01, one-way ANOVA.

(E) KEGG pathway analysis was used to examine differentially expressed genes between the control and Deg-AZM-treated HISMCs. Deg-AZM increased the expression of genes related to smooth muscle contraction and metabolism.

(F) HISMCs were harvested after treatment with 0 (lane 1, 4), 20 (lane 2, 5), and 40 μM (lane, 3, 6) Deg-AZM solutions. G-actin and F-actin were fractionated from HISMCs and assessed through western blot analysis. The F-actin:G-actin ratio was calculated in accordance with the densitometry analysis results for western blots. **p < 0.01, one-way ANOVA.

(G) Negative staining electron microscopy images of actin alone, actin with transgelin, and actin with transgelin and Deg-AZM.

(H) Detailed statistical results for negative staining electron microscopy assays. Statistical indicators included the total length of F-actin, the average length of F-actin, and the area of F-actin in each group. **p < 0.01, one-way ANOVA. Each bar represents the mean ± SD for biological triplicate experiments.

Deg-AZM Can Promote Actin Polymerization and Actin Filament Assembly

Confocal experiments confirmed that the location of Deg-AZM and the location of transgelin in HISMCs was colocalized. The values of the Pearson's correlation coefficient and Mander's overlap of Deg-AZM and transgelin were 0.882 and 0.884, respectively. Single-molecule imaging (stochastic optical reconstruction microscopy, STORM) further confirmed that Deg-AZM colocalized with transgelin. Furthermore, Deg-AZM molecules that overlapped with transgelin were distributed along the microfilament (Figure 6A). Transgelin, an actin-binding protein, can interact with actin filaments during the organization of actin cytoskeletons in human intestinal SMCs (HISMCs). Additional transgelin molecules colocalized with actin as Deg-AZM concentration was increased (Figure 6B). Deg-AZM can reduce the lengths of HISMCs in a dose-dependent manner (Figure 6B). The results of the Deg-AZM versus vincristine experiment show that Deg-AZM can increase the stability and bundling of actin filaments by promoting the interaction between transgelin and actin and reducing the depolymerization effect of vincristine (Figure 6C). We measured the concentrations of reactive oxygen species (ROS), lactate dehydrogenase (LDH), and adenosine triphosphate (ATP) in control and Deg-AZM-treated HISMCs. ATP consumption was increased with respect to the Deg-AZM concentration, whereas ROS and LDH consumption remained basically unchanged (Figure 6D). These results suggest that Deg-AZM indeed increased the contraction of intestinal SMCs without any severe side effects. Functional enrichment of upregulated genes in Deg-AZM-treated smooth muscle cells was analyzed. Gene set enrichment analysis (GSEA) results indicated that Deg-AZM enhanced the contractile capacity of SMCs through the positive regulation of actin cytoskeleton reorganization, filopodium assembly, and efficient energy use (Figures 6E and S12 and Table S3).

We harvested HISMCs at 24 h after treatment with 0, 20, and 40 μM Deg-AZM to examine if Deg-AZM can promote the polymerization of G-actin to F-actin. G-actin and F-actin were separated from HISMCs through lysis buffer treatment and centrifugation, and western blot was used to analyze actin content. Deg-AZM treatment promoted actin polymerization and increased the F-actin:G-actin ratio as determined by western Blot analysis with actin antibodies (Figure 6F). We also performed cryoelectron microscopy (cryoEM) to observe F-actin filaments after treatment with Deg-AZM. Actin filaments appeared short and unbundled in the absence of transgelin. A high number of long F-actin filaments formed in the presence of transgelin. Additional F-actin filaments and F-actin filament bundles were observed after treatment with Deg-AZM (Figure 6G). Thus, Deg-AZM may bind to transgelin, stabilize actin filaments, and increase the number of F-actin filament bundles. The detailed parameters of F-actin filaments seen under cryoEM are listed in Figure 6H. The F-actin area, F-actin percentage area, total F-actin length, and average F-actin length in the Deg-AZM-treated group increased.

We performed molecular docking and dynamic simulations to predict the binding mode of Deg-AZM to transgelin. Deg-AZM bound to the transgelin active site with the highest number of hydrogen bonding interactions and the lowest binding energy. The docking score of Deg-AZM binding to transgelin was −3.548. The binding energy of transgelin and actin was −123.55 kcal/mol under the Deg-AZM effect (Table S4). Overall, Deg-AZM bound to transgelin.

Deg-AZM Does Not Exert a Therapeutic Effect in Transgelin Knockout Mice

We tested the intestinal motility of Deg-AZM in a transgelin knockout animal model (Figure 7A). Transgelin knockout mice were C57 mice, and transgelin knockout did not affect the health of the mice. Deg-AZM did not affect intestinal peristalsis in the transgelin knockout constipation mouse models induced with atropine
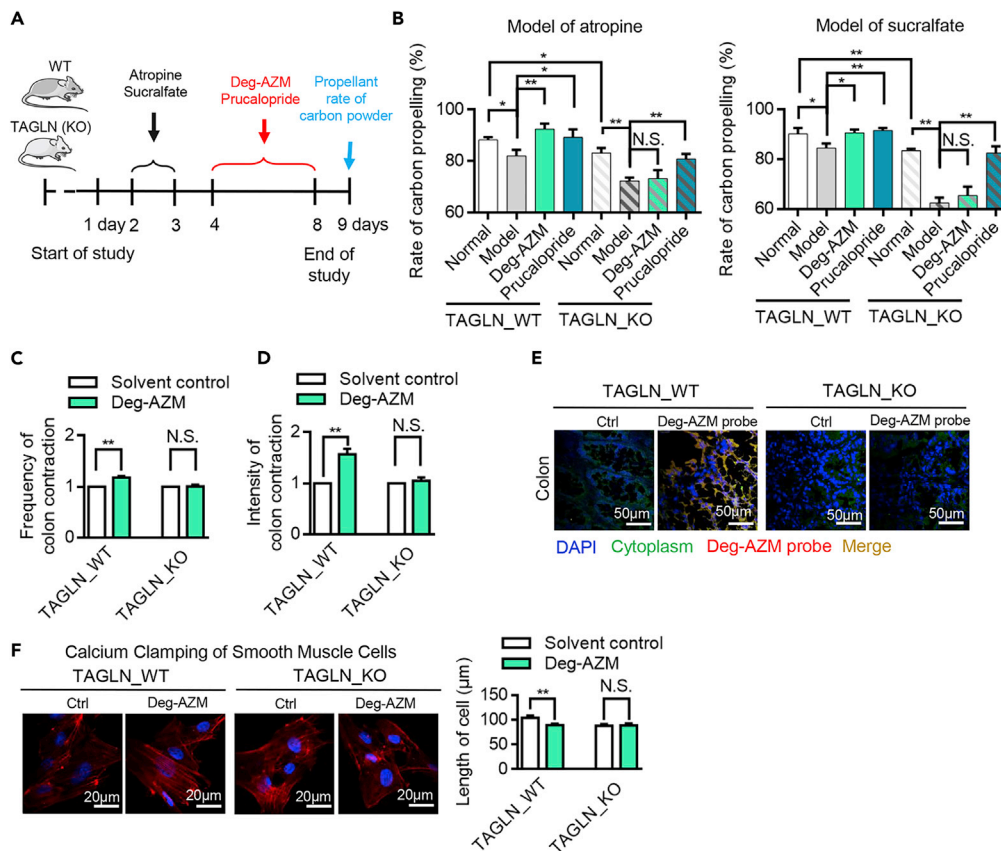
Figure 7. Transgelin Is Verified as the Target of Deg-AZM in Transgelin Knockout Mice

(A) Schematic of the experimental procedure for the construction of the wild-type animal constipation model and transgelin knockout mice.

(B) Determination of intestinal motility of Deg-AZM in wild-type and transgelin knockout mice. Deg-AZM showed significant effects on carbon propelling power in wild-type mice but minimal effects on carbon propelling power in transgelin knockout mice. **$p < 0.01$, one-way ANOVA.

(C) Contraction intensity of isolated intestinal tissues from two animal models were measured *in vitro*. **$p < 0.01$, *Student's t test*.

(D) Contraction frequency of isolated intestinal tissues from two animal models were measured *in vitro*. Deg-AZM showed intense effects on tissues from the wild-type model but minimal effects on tissues from transgelin knockout mice. **$p < 0.01$, Student's t test.

(E) Colonic tissue staining results of Deg-AZM fluorescent probes in wild-type and transgelin knockout mice. No evident Deg-AZM probe was found in the colon tissues of transgelin knockout mice fed with Deg-AZM probes.

(F) Calcium clamping results showed that Deg-AZM cannot increase intestinal smooth muscle contraction in transgelin knockout cells. **$p < 0.01$, Student's t test. Each bar represents the mean $\pm$ SD for different animal measurements.

and sucralfate (Figure 7B). Colon muscle tension measurements showed that Deg-AZM did not affect transgelin knockout tissue (Figures 7C and 7D). Deg-AZM was positively stained by its antibody in wild-type colon tissue but was negatively stained in transgelin knockout colon tissue (Figure 7E). Calcium-clamping experiments also revealed that Deg-AZM promotes the contraction of colonic SMCs and reduces cell length but not that of transgelin knockout cells (Figure 7F).

Deg-AZM Lacks Antibacterial Activity

Although AZM can increase intestinal peristalsis, it is not used to treat constipation because of its antibacterial activity. Antibacterial experiments showed that Deg-AZM lost the inhibitory effect of AZM on different bacteria, including pathogenic (*Staphylococcus aureus*, *Pseudomonas aeruginosa*, and *Monilia albicans*) and normal bacteria (*Bacillus bifidus*, *Bacillus acidi lactici*, and *Escherichia coli*) (Figure 8A). Mouse fecal samples were subjected to 16S rDNA sequencing after 4 weeks of Deg-AZM administration. We
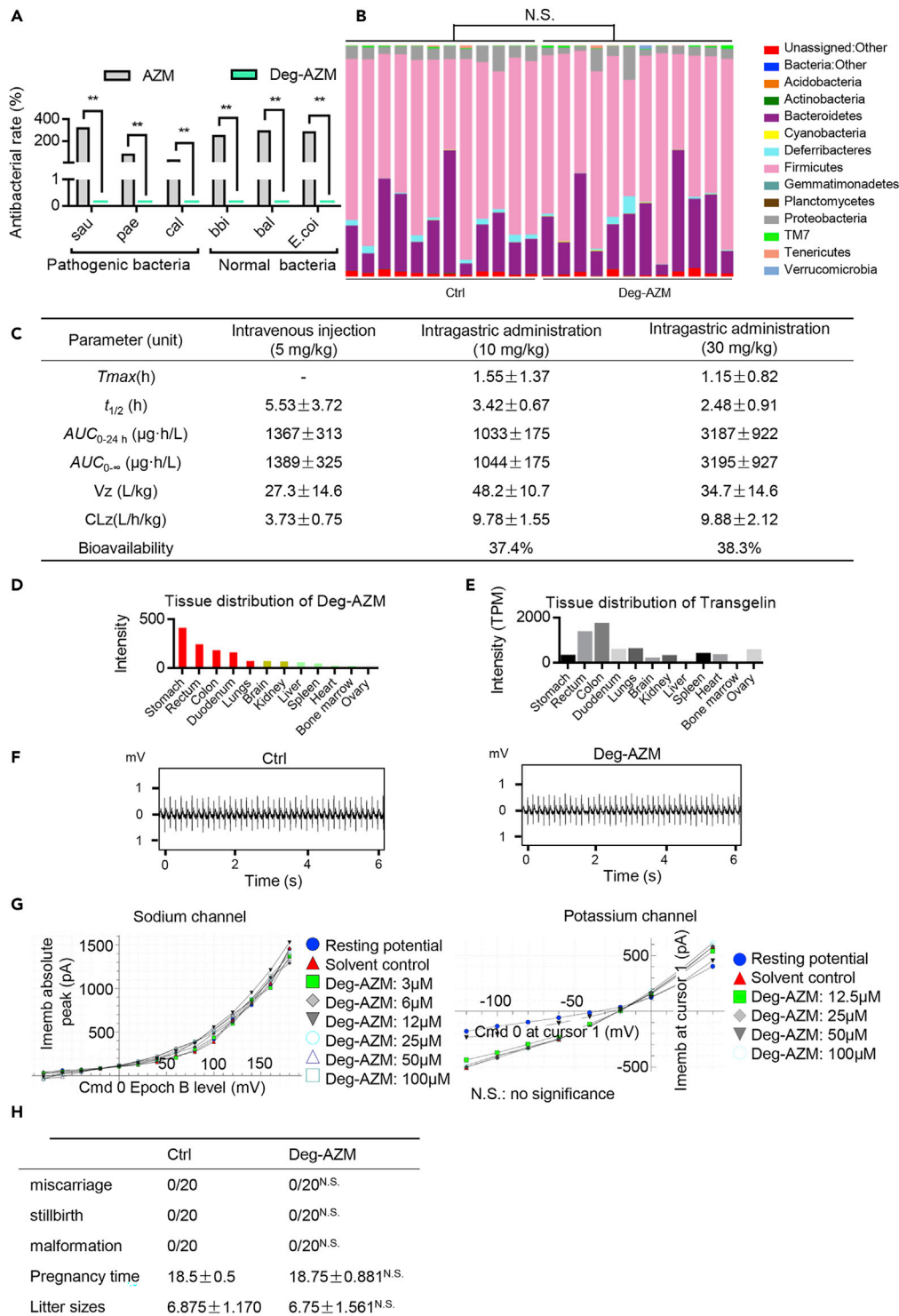
Figure 8. Deg-AZM Shows No Toxicity toward Animals and Lacks Antibacterial Activity

(A) Test of the antibacterial activity of Deg-AZM against pathogenic and normal bacteria. **p < 0.01, Student's t test.

(B) Intestinal flora in fecal samples from the control (normal) and Deg-AZM-treated groups were sequenced. No significant differences in the distribution of bacterial types between control and Deg-AZM-treated samples.

(C) Harmacokinetics data for different doses of Deg-AZM.

(D) Tissue distribution of Deg-AZM in mice.

Figure 8. *Continued*

(E) Data for transgelin distribution in various organs were obtained from the Human Gene Database (http://www.genecards.org).

(F) Cardiac toxicity of Deg-AZM in mice was measured through ECG. Deg-AZM did not exert cardiac toxicity.

(G) Sodium and potassium ion channel excitant activities by Deg-AZM were measured in the calcium clamping of SMC. No evident excitation was observed.

(H) Uterine stimulation by Deg-AZM in mice at different pregnancy stages was tested. Deg-AZM had no side effects on pregnant mice. Student's t test. Each bar represents the mean $\pm$ SD for biological triplicate experiments or different animal measurements.

confirmed that Deg-AZM lacked any antibacterial activity. Subsequent cluster, principal component, and Shannon analyses showed no significant difference in bacterial flora between the control and Deg-AZM-treated groups (Figures S13 and S14). Further analysis showed a balanced proportion of micro-flora at the phylum levels (Figure 8B).

Deg-AZM Lacked Major Toxicity *In Vivo*

We investigated the pharmacokinetics of Deg-AZM in rats that received single doses of Deg-AZM through intravenous or intragastric administration. Blood samples were collected from the retrobulbar venous plexus of the rats. The plasma concentration–time curve of the rats that received 5 mg/kg Deg-AZM through intravenous injection is shown in Figure S14A. The plasma concentration–time curves of rats that received 10 and 30 mg/kg Deg-AZM through intragastric administration are shown in Figures S14B and S14C, respectively. Pharmacokinetics and pharmacodynamics data are provided in 8C. The half-lives of Deg-AZM administered through intravenous and intragastric routes at the doses of 10 and 30 mg/kg were 3.42 and 2.48 h. The bioavailabilities of Deg-AZM in groups that received 10 and 30 mg/kg Deg-AZM through intragastric administration were 37.4% and 38.3%, respectively. Drug acute toxicity, long-term toxicity, and reproductive toxicity were tested, and no abnormalities were found (Figures S15D and S15E).

Tissue distribution measurement showed that Deg-AZM was mainly distributed in the stomach and intestine and was slightly distributed in the uterus and heart (Figure 8D). Transgelin was highly expressed in colon tissue but can also be seen in the ovary and heart (data were downloaded from the human protein atlas: https://www.proteinatlas.org) (Figure 8E). The cardiac toxicity of Deg-AZM was tested by using electrocardiograms (ECGs). The ECGs of mice in the control and Deg-AZM-treated groups showed negligible differences (Figure 8F). Electrophysiological studies indicate that Deg-AZM treatment did not significantly change the sodium and potassium channels of HISMCs (Figure 8G). To further verify that Deg-AZM was not cardiotoxic, we determined the cardiotoxicity of Deg-AZM by using the HEK293 cell line with stable expression of the hERG potassium channel. In this study, patch-clamp technique was used to detect the concentration effect relationship of Deg-AZM on blocking the hERG channel, so as to evaluate the risk of Deg-AZM inhibiting the hERG potassium channel in the heart. Experimental results show that Deg-AZM has no obvious suppression effect on hERG potassium channel (Table S5). We treated 16-day pregnant mice (n = 20) with Deg-AZM by intragastric administration to test if Deg-AZM can cause uterine irritation and miscarriage. No premature births, abortions, or deformities were observed among the treated mice (Figure 8H). Furthermore, the results of our cytotoxicity test showed that Deg-AZM lacked toxicity toward 293T, MDCK, 293, and 3T3 cell lines (Figure S16). Therefore, Deg-AZM may be a safe lead compound for consti-pation treatment.

DISCUSSION

AZM, a macrolide, is commonly used to treat chronic pseudo-obstruction and diabetic gastroparesis and to promote gastrointestinal motility (Barboza et al., 2015; Chini et al., 2012). Gastrointestinal reactions are the most common adverse reactions caused by AZM (Wang et al., 2005). AZM can also increase plasma motilin levels (Broad and Sanger, 2013). Subsequently, the binding of motilin to gastric motility receptors on gastrointestinal smooth muscles produces strong contractions that induce abnormal gastrointestinal reactions, such as pain, nausea, and vomiting (Barboza et al., 2015) (Broad and Sanger, 2013). AZM is extremely unstable in acidic conditions, and the majority of AZM is degraded after stomach passage. However, the mechanism underlying the ability of AZM to induce strong intestinal peristalsis remains unclear. Children who received AZM through oral administration had more severe AZM-related gastrointestinal adverse reactions than those who received AZM via injection (p < 0.05) (Zhang and Wei, 2014). Our recent

pharmacology studies show that the intestinal side effects of AZM may be caused by one of its metabolites, that is, Deg-AZM.

In contrast to AZM, Deg-AZM binds to transgelin instead of the motilin receptor. Transgelin is a 201-amino-acid peptide that belongs to the calponin family of actin-binding proteins. It has an N-terminal calponin homologue domain (CH) and a single C-terminal calponin-like module. The CLIK domain is required for actin binding and can be found throughout the normal smooth muscles of adult vertebrates (Assinder et al., 2009). The transgelin family consists of transgelin-1, -2, and -3, which have the same molecular weights but different isoelectric points (pI 9.0, 8.4, and 7.0) (Assinder et al., 2009; Daniel et al., 2012; Lee et al., 2010; Yin et al., 2018). Each transgelin subtype is expressed in different organs. Transgelin-1 is mainly expressed in visceral and vascular SMCs, and transgelin-2 is expressed in most cell types, including SMCs to immune cells (Zhong et al., 2018). It is mainly expressed in the bronchial epithelium, lung mesenchyme, and gastrointestinal epithelium, as well as in the cartilaginous and periosteal layers of bones, but not in the SMC of muscle mucosa in the gastrointestinal tract (Aldeiri et al., 2018; Pape et al., 2008; Zhang et al., 2002). Meanwhile, transgelin-3 is mainly found in the nervous system. Target retrieval result display, Deg-AZM, binds to transgelin-1, which is widely expressed in intestinal SMCs (Figure 5C). Deg-AZM further enhances transgelin binding to actin and facilitates F-actin formation. Transgelin also plays a significant role in the reorganization of F-actin filaments into actin filament bundles as observed in our cryoEM experiments (Figure 6G). Actin filament bundles further form stress fibers with myosin in SMCs (Thompson et al., 2012; Tojkander et al., 2012). Stress fibers are the major contractile structures in many animal cells. In summary, Deg-AZM can increase G-actin polymerization and F-actin filament assembly by binding to transgelin. It can increase the formation and stability of F-actin, F-filament bundles, and stress fibers, thus ultimately increasing the contractile capacity of intestinal SMCs (Mogilner and Oster, 1996; Pollard and Borisy, 2003). This conclusion was proved by our results for mouse transgelin (−/−) constipation models (Figure 7). Treatment with Deg-AZM failed to increase intestinal peristalsis in mouse transgelin (−/−) constipation models but not in wild-type mouse models. The administration of Deg-AZM does not reduce the expression of Transgelin, so Deg-AZM may not cause rapid tachyphylaxis.

Deg-AZM can also prevent gastrointestinal motility retrogradation and gastroesophageal reflux given that it binds to transgelin instead of motilin receptors (Leming et al., 2011; Ozaki et al., 2009; Sanger et al., 2009). It lacks antibacterial activity and does not disrupt intestinal flora *in vivo*. In addition, we tested the cardiovascular toxicity and uterine stimulation effects of Deg-AZM given that transgelin-1 is expressed mainly in visceral and vascular smooth muscle. Deg-AZM lacked cardiovascular toxicity and uterine stimulation effects because it was present at low concentrations in the heart and the uterus (Figure 8D). Long-term toxicity studies failed to find significant changes in body weight (BW), general condition, and behavior between the control and Deg-AZM-treated groups. Deg-AZM may be a good therapeutic candidate for constipation treatment. Transgelin, the target of Deg-ASM, may have therapeutic applications as an effective enhancer of intestinal smooth muscle contraction.

Limitations of the Study
This study evaluated the therapeutic effect of Deg-AZM on animal models of constipation. At the same time, Deg-AZM was found to promote intestinal smooth muscle cell contraction by targeting transgelin to treat constipation. Further evaluation of Deg-AZM or azithromycin derivatives in the treatment of gastroparesis is also of great significance. Transgelin agonists can also be further developed.

Resource Availability
Lead Contact
Further information and requests for resources and reagents should be directed to and will be fulfilled by the Lead Contact, Dr. Tao Sun (sunrockmia@hotmail.com).

Material Availability
All unique/stable reagents generated in this study are available from the Lead Contact on reasonable request.

Data and Code Availability
The accession number for the data reported in this paper is GEO: GSE156032.

AUTHOR CONTRIBUTIONS

C.Y., T.S., H.Z., and B.W. designed research. W.Z., B.S., G.Y., B.Q, H.C., H.R., L.H., and Y.F. performed research and analyzed data. A.R., X.H., Y.L., X.L., Q.Y., and T.Y. performed data analysis. W.Z., L.H., and B.S. wrote the paper, with contributions from all authors.

DECLARATION OF INTERESTS

The authors declare no conflict of interests.

REFERENCES

Aldeiri, B., Roostalu, U., Albertini, A., Behnsen, J., Wong, J., Morabito, A., and Cossu, G. (2018). Abrogation of TGF-beta signalling in TAGLN expressing cells recapitulates Pentalogy of Cantrell in the mouse. Sci. Rep. 8, 3658.

Assinder, S.J., Stanton, J.A., and Prasad, P.D. (2009). Transgelin: an actin-binding protein and tumour suppressor. Int. J. Biochem. Cell Biol. 41, 482–486.

Barboza, J.L., Okun, M.S., and Moshiree, B. (2015). The treatment of gastroparesis, constipation and small intestinal bacterial overgrowth syndrome in patients with Parkinson's disease. Expert Opin. Pharmacother. 16, 2449–2464.

Broad, J., and Sanger, G.J. (2013). The antibiotic azithromycin is a motilin receptor agonist in human stomach: comparison with erythromycin. Br. J. Pharmacol. 168, 1859–1867.

Chini, P., Toskes, P.P., Waseem, S., Hou, W., McDonald, R., and Moshiree, B. (2012). Effect of azithromycin on small bowel motility in patients with gastrointestinal dysmotility. Scand. J. Gastroenterol. 47, 422–427.

Corvaglia, L., Faldella, G., Rotatori, R., Lanari, M., Capretti, M.G., and Salvioli, G.P. (2004). Intrauterine growth retardation is a risk factor for cisapride-induced QT prolongation in preterm infants. Cardiovasc. Drugs Ther. 18, 371–375.

Daniel, C., Ludke, A., Wagner, A., Todorov, V.T., Hohenstein, B., and Hugo, C. (2012). Transgelin is a marker of repopulating mesangial cells after injury and promotes their proliferation and migration. Lab Invest. 92, 812–826.

Depoortere, I., Peeters, T.L., and Vantrappen, G. (1990). Development of motilin receptors and of motilin- and erythromycin-induced contractility in rabbits. Gastroenterology 99, 652–658.

Deruyttere, M., Lepoutre, L., Heylen, H., Samain, H., and Pennoit, H. (1987). Cisapride in the management of chronic functional dyspepsia: a multicenter, double-blind, placebo-controlled study. Clin. Ther. 10, 44–51.

Drolet, B., Khalifa, M., Daleau, P., Hamelin, B.A., and Turgeon, J. (1998). Block of the rapid component of the delayed rectifier potassium current by the prokinetic agent cisapride underlies drug-related lengthening of the QT interval. Circulation 97, 204–210.

Elsafadi, M., Manikandan, M., Dawud, R.A., Alajez, N.M., Hamam, R., Alfayez, M., Kassem, M., Aldahmash, A., and Mahmood, A. (2016). Transgelin is a TGFbeta-inducible gene that regulates osteoblastic and adipogenic differentiation of human skeletal stem cells through actin cytoskeleton organization. Cell Death Dis. 7, e2321.

Johanson, J.F. (2004). Review article: tegaserod for chronic constipation. Aliment. Pharmacol. Ther. 20 (Suppl 7), 20–24.

Johanson, J.F., Wald, A., Tougas, G., Chey, W.D., Novick, J.S., Lembo, A.J., Fordham, F., Guella, M., and Nault, B. (2004). Effect of tegaserod in chronic constipation: a randomized, double-blind, controlled trial. Clin. Gastroenterol. Hepatol. 2, 796–805.

Kav, T., and Bayraktar, Y. (2010). Herbal remedies are the main etiologic factor in melanosis coli, a case series study. Open Med. 5, 347–353.

Kim, J.E., Koh, E.K., Song, S.H., Sung, J.E., Lee, H.A., Lee, H.G., Choi, Y.W., and Hwang, D.Y. (2017). Effects of five candidate laxatives derived from Liriope platyphylla on the 5-HT receptor signaling pathway in three cell types present in the transverse colon. Mol. Med. Rep. 15, 431–441.

Lee, E.K., Han, G.Y., Park, H.W., Song, Y.J., and Kim, C.W. (2010). Transgelin promotes migration and invasion of cancer stem cells. J. Proteome Res. 9, 5108–5117.

Lees-Miller, J.P., Heeley, D.H., and Smillie, L.B. (1987a). An abundant and novel protein of 22 kDa (SM22) is widely distributed in smooth muscles. Purification from bovine aorta. Biochem. J. 244, 705–709.

Lees-Miller, J.P., Heeley, D.H., Smillie, L.B., and Kay, C.M. (1987b). Isolation and characterization of an abundant and novel 22-kDa protein (SM22) from chicken gizzard smooth muscle. J. Biol. Chem. 262, 2988–2993.

Leming, S., Broad, J., Cozens, S.J., Otterson, M., Winchester, W., Lee, K., Dukes, G.E., and Sanger, G.J. (2011). GSK962040: a small molecule motilin receptor agonist which increases gastrointestinal motility in conscious dogs. Neurogastroenterol. Motil. *23*, 958–e410.

Malagelada, C., Nieto, A., Mendez, S., Accarino, A., Santos, J., Malagelada, J.R., and Azpiroz, F. (2017). Effect of prucalopride on intestinal gas tolerance in patients with functional bowel disorders and constipation. J. Gastroenterol. Hepatol. *32*, 1457–1462.

Mansour, N.M., Ghaith, O., El-Halabi, M., and Sharara, A.I. (2012). A prospective randomized trial of mosapride vs. placebo in constipation-predominant irritable bowel syndrome. Am. J. Gastroenterol. *107*, 792–793.

Mogilner, A., and Oster, G. (1996). Cell motility driven by actin polymerization. Biophys. J. *71*, 3030–3045.

Moshiree, B., McDonald, R., Hou, W., and Toskes, P.P. (2010). Comparison of the effect of azithromycin versus erythromycin on antroduodenal pressure profiles of patients with chronic functional gastrointestinal pain and gastroparesis. Dig. Dis. Sci. *55*, 675–683.

Ozaki, K., Onoma, M., Muramatsu, H., Sudo, H., Yoshida, S., Shiokawa, R., Yogo, K., Kamei, K., Cynshi, O., Kuromaru, O., et al. (2009). An orally active motilin receptor antagonist, MA-2029, inhibits motilin-induced gastrointestinal motility, increase in fundic tone, and diarrhea in conscious dogs without affecting gastric emptying. Eur. J. Pharmacol. *615*, 185–192.

Pape, M., Doxakis, E., Reiff, T., Duong, C.V., Davies, A., Geissen, M., and Rohrer, H. (2008). A function for the calponin family member NP25 in neurite outgrowth. Dev. Biol. *321*, 434–443.

Pollard, T.D., and Borisy, G.G. (2003). Cellular motility driven by assembly and disassembly of actin filaments. Cell *112*, 453–465.

Potter, T.G., and Snider, K.R. (2013). Azithromycin for the treatment of gastroparesis. Ann. Pharmacother. *47*, 411–415.

Sanger, G.J., and Furness, J.B. (2016). Ghrelin and motilin receptors as drug targets for gastrointestinal disorders. Nat. Rev. Gastroenterol. Hepatol. *13*, 38–48.

Sanger, G.J., Westaway, S.M., Barnes, A.A., Macpherson, D.T., Muir, A.I., Jarvie, E.M., Bolton, V.N., Cellek, S., Naslund, E., Hellstrom, P.M., et al. (2009). GSK962040: a small molecule, selective motilin receptor agonist, effective as a stimulant of human and rabbit gastrointestinal motility. Neurogastroenterol Motil. *21*, 657–664, e630-651.

Satoh, Y., Sugiyama, A., Tamura, K., and Hashimoto, K. (2000). Effects of mexiletine on the canine cardiovascular system complicating cisapride overdose: potential utility of mexiletine for the treatment of drug-induced long QT syndrome. Jpn. J. Pharmacol. *83*, 327–334.

Shah, E.D., Kim, H.M., and Schoenfeld, P. (2018). Efficacy and tolerability of guanylate cyclase-C agonists for irritable bowel syndrome with constipation and chronic idiopathic constipation: a systematic review and meta-analysis. Am. J. Gastroenterol. *113*, 329–338.

Sharma, A., and Rao, S. (2017). Constipation: pathophysiology and current therapeutic approaches. Handb Exp. Pharmacol. *239*, 59–74.

Shen, H. (2009). Discussion on certain issues of the diagnosis and treatment of functional constipation. Chin. J. Integr. Med. *15*, 89.

Thompson, O., Moghraby, J.S., Ayscough, K.R., and Winder, S.J. (2012). Depletion of the actin bundling protein SM22/transgelin increases actin dynamics and enhances the tumourigenic phenotypes of cells. BMC Cell Biol. *13*, 1.

Tojkander, S., Gateva, G., and Lappalainen, P. (2012). Actin stress fibers–assembly, dynamics and biological roles. J. Cell Sci. *125*, 1855–1864.

Ueno, N., Inui, A., and Satoh, Y. (2010). The effect of mosapride citrate on constipation in patients with diabetes. Diabetes Res. Clin. Pract. *87*, 27–32.

Van Outryve, M., Nutte, N.D., Van Eeghem, P., and Gooris, J. (1993). Efficacy of cisapride in functional dyspepsia resistant to domperidone or metoclopramide: a double-blind, placebo-controlled study: general discussion. Scand. J. Gastroenterol. *28*, 47–53.

Wang, S.H., Lin, C.Y., Huang, T.Y., Wu, W.S., Chen, C.C., and Tsai, S.H. (2001). QT interval effects of cisapride in the clinical setting. Int. J. Cardiol. *80*, 179–183.

Wang, X., Du, W., and Wang, H. (2005). Analysis of 164 reported adverse drug reactions of azithromycin. China J. Mod. Med. 1550–1552.

Yin, L.M., Xu, Y.D., Peng, L.L., Duan, T.T., Liu, J.Y., Xu, Z., Wang, W.Q., Guan, N., Han, X.J., Li, H.Y., et al. (2018). Transgelin-2 as a therapeutic target for asthmatic pulmonary resistance. Sci. Transl. Med. *10*, 1–10.

Zhang, J.C., Helmke, B.P., Shum, A., Du, K., Yu, W.W., Lu, M.M., Davies, P.F., and Parmacek, M.S. (2002). SM22beta encodes a lineage-restricted cytoskeletal protein with a unique developmentally regulated pattern of expression. Mech. Dev. *115*, 161–166.

Zhang, L., and Wei, X. (2014). High risk factors of azithromycin-related gastrointestinal adverse reaction in children. J. Pediatr. Pharm. 50–52.

Zhong, W., Sun, B., Gao, W., Qin, Y., Zhang, H., Huai, L., Tang, Y., Liang, Y., He, L., Zhang, X., et al. (2018). Salvianolic acid A targeting the transgelin-actin complex to enhance vasoconstriction. EBioMedicine *37*, 246–258.

Zhou, H.M., Fang, Y.Y., Weinberger, P.M., Ding, L.L., Cowell, J.K., Hudson, F.Z., Ren, M., Lee, J.R., Chen, Q.K., Su, H., et al. (2016). Transgelin increases metastatic potential of colorectal cancer cells in vivo and alters expression of genes involved in cell motility. BMC Cancer *16*, 55.

Supplemental Information

Deglycosylated Azithromycin Targets Transgelin

to Enhance Intestinal Smooth Muscle Function

Weilong Zhong, Bo Sun, Hao Ruan, Guang Yang, Baoxin Qian, Hailong Cao, Lingfei He, Yunjing Fan, Arthur G. Roberts, Xiang Liu, Xuejiao Hu, Yuan Liang, Qing Ye, Tingting Yin, Bangmao Wang, Cheng Yang, Tao Sun, and Honggang Zhou

Transparent Methods

Patient Samples

Thirty-eight human volunteers (including 22 males and 16 females, with a mean age of 26.0±3.3 years) were recruited to receive AZM daily so that their intestinal motility could be measured and that their fecal samples could be analyzed for the presence of Deg-AZM. Then, 36 patients (including 29 males and 7 females, with a mean age of 57.9±12.1) with chronic constipation were recruited. The volunteers had no general complaints about the difficulty or frequency of defecation and abdominal discomfort or pain. The ROME IV criteria were utilized to diagnose if the patients had chronic constipation, and abdominal pain was set as an exclusion criterion. All the volunteers and patients involved in this study signed the informed consent, and the study program was approved by the theoretical committee of the Tianjin Third Central Hospital.

Intestinal SMC culture. HISMCs were purchased from CHI Scientific (Jiangsu, China). Intestinal SMCs were cultured in DMEM and then passaged after enzyme digestion. The test was repeated after the cell culture had stabilized.

AZM, loperamide, atropine, and prucalopride. AZM, loperamide, and atropine were purchased from Dalian Meilun Biology Technology Co., Ltd. Prucalopride was obtained from Shanghai Famo Biotechnology Co., Ltd.

Animals. SPF mice weighing 18–22 g were obtained from Vital River Laboratory Animal Technology Co., Ltd. (Beijing, China). The diets provided to the animals in this study were experimental animal-specific food purchased from Beijing Huafukang biotechnology co., LTD., and feed ingredients of the animals in each group were consistent. Nutrients of feed are shown in Table S1. All animals had free access to standard lab chow and water. Laboratory animal license (number of animal license SYXK (JIN) 2017-0003).

Transgelin-knockout animal models. The animal experiment was performed in accordance with the guiding principles of the Institutional Animal Care and Use Committee. Transgelin (−/−) C57/BL6 mice were obtained from Jackson Laboratories (Bar Harbor, ME, USA). The intestinal peristalsis assay of transgelin-knockout mice was performed as described above.

Mouse constipation model induced by atropine and sucralfate. The atropine and sucralfate was used to induce constipation in mouse according to previous reports(Bazanova et al., 1954). Breifly, after quarantine, all mice were randomly divided into control, model, prucalopride, AZM, AZM-1 and Deg-AZM groups (n = 6). The behaviors and statuses of the mice were observed on day 1. The mice in the model groups received 15 mg/kg BW atropine and 5 mg/kg BW sucralfate twice daily through oral administration on days 2 and 3. The mice in the normal control group received 0.9% sodium chloride. The mice were allowed free access to water and fasted for 30 min before administration on days 4–8. Then, the normal and model groups received 0.9% sodium chloride, whereas the prucalopride group was treated with 0.3 mg/kg prucalopride. Meanwhile, the AZM group were treated with 75 mg/kg AZM. Deg-AZM was treated with 80 mg/kg. Other groups received a corresponding dose of the tested compounds. The low, medium and high dose Deg-AZM group was given 21.7, 43.4 and 86.8 mg/kg respectively. All mice were fasted for 30 min on day 9. Then, all mice received 0.2 mL of 5% charcoal powder suspended in 10% gum arabic solution through oral administration. The mice were sacrificed at 90 min after charcoal powder administration and dissected. The cardia to the rectum were collected. The length of the cardia to the rectum and the distance between carbon powders to cardia were measured. Measuring the length of charcoal propulsion (pyloric to charcoal the distance from the distal anterior edge) and the length of the small intestine (the distance from the pylorus to the ileocecal area) were calculated for the rate of propulsion of the carbon.

Charcoal propulsion rate = distance from pyloric to charcoal front (cm) / small intestine length (cm) × 100%

Pharmacodynamic experiments on Deg-AZM in rabbits, dogs, and monkeys. The animals were allocated into the control and experimental groups (n = 5). The control group received normal diets, whereas the experimental group was fed with Deg-AZM. The rabbit, dog, and monkey groups received 1.94, 1.1, and 0.62 mg/kg Deg-AZM, respectively, in accordance with the animal surface area. Each animal and food were weighed, and Animal feces were collected within 24 h. Fecal pellets were counted and weighed.

Determination of the localization of AZM, EM, and Deg-AZM in different gastrointestinal organs. Healthy mice were sacrificed, and their stomachs, jejunums, ilea, ceca, and colons were collected and washed with 1× PBS. Tissue samples were embedded with OTC agent. Tissue slices were then frozen. Frozen sections were fixed with 75% ethanol for 10 min and then separately incubated with 20 μM AZM, EM, and Deg-AZM probes and the linker control at room temperature for 2 h. The sections were removed from the incubation solution, washed twice for 10 min with 1× PBS, and then irradiated with UV with the wavelength of 350 nm for 30 min. Antigen blocking was performed with 100 μL of 2% BSA for 1 h. The sections were washed twice with cold PBS for 5 min and then incubated with 100 μL aliquots of fresh click reaction solution consisting of 1 mM $CuSO_4$, 1 mM TCEP, 100 μM TBTA, and 10 μM rhodamine-N_3 at room temperature for 2 h. Then, the sections were treated with endoplasmic reticulum probe (ER-green) for 20 min at 37 °C. ER-green working fluid was removed, and the sections were washed twice with PBS. Afterward, DAPI-dyed nuclei were imaged by using a confocal microscope (Nikon, Japan).

***In vivo* location of AZM, EM, and Deg-AZM at different time points.** Healthy mice were fasted for 12 h and then fed with 5 mg/kg AZM probe, EM probe, Deg-AZM probe, and linker control probes. The same experiment was repeated thrice. The mice were sacrificed after 2, 4, 8, and 12 h. The stomach, jejunum, ileum, cecum, and colon of each mouse were obtained, cleaned, and washed with 1× PBS. Then, stained probe immunofluorescence was performed in accordance with the abovementioned steps.

Muscular tension measurement of intestinal and gastric smooth muscles.

The tension signal was measured using the DA100C amplifier. The amplifier gain was set at 1,000, the high-pass filter was set in DC, and the low-pass filter was set at 10 Hz. The tension transducer was calibrated prior to use. Female mice were selected after calibration and anesthetized with pentobarbital sodium (50 mg/kg, Sigma, USA) to collect the stomach and intestinal segments. One end of the intestine was fixed on the hook of the tension transducer, and another end of the intestine was fixed on the fixed object. Subsequently, the intestine was immersed in Tyrode's solution at 37 °C. The contractile tension of the longitudinal muscles was measured using a polyconductive

physiometer (MP150, Biopac system, Inc., USA). Tension waveform collection was initiated upon intestinal fixation. The intestine was first treated with solvent and then with 20 μM Deg-AZM. Gastric tissue muscle tension was measured in a similar manner.

Identification of the molecular target of Deg-AZM. Healthy mice were sacrificed, and the stomachs, duodenums, ilea, ceca, and colons were collected and washed twice with prechilled 1× PBS. Next, the tissues were ground with liquid nitrogen. Afterward, 400 μL of tissue lysate (containing 1 mM PMSF) was placed on ice for 30 min. Exactly 200 μL of DNA lysis buffer was added to the protein lysate. The mixture was incubated for 1 h at 37 °C and then centrifuged at 20,000 g under 4 °C for 10 min. The pellet was discarded, and the protein supernatant was aspirated into a new EP tube. The Deg-AZM probe and linker control were coincubated with protein for 5 h. The final probe concentration was 50 μM. The incubation solution was irradiated with a UV lamp at a wavelength of 350 nm for 30 min. The protein solution was mixed with click reaction solution and incubated on ice for 2 h. The reacted protein solution was loaded with 1× loading buffer (no SDS) and then separated on 12% native-PAGE gel. The differential fluorescent bands were separated, hydrolyzed, and subjected to mass spectrometry.

Surface plasmon resonanceassay of Deg-AZM binding to transgelin. Transgelin was fixed on the chip surface, which was then activated with PBS-EP buffer in accordance with the standard EDC/N-hydroxysuccinimide (NHS) protocol. Residual active groups were inactivated through injection with 1.15 mg/mL transgelin for 12 min and then with 1 M ethanolamine at pH 8.5 for 7 min. Approximately 4,000 RU of transgelin was fixed in a typical reaction. Deg-AZM solutions were diluted to concentrations of 12.5, 25, 50, 150, and 200 μM. Insoluble residues were pelleted through centrifugation and then discarded. Exactly 200 μL of the supernatant was input at 30 μL/min flow rate. The protein binding time was set as 180 s, and the dissociation time was set as 300 s. Dynamic analysis data were calculated using BIAevaluation software.

Microscale thermophoresis. Transgelin lysine residues were labeled in accordance with the protocol for the NHS coupling of the NT647 fluorescence dye (NanoTemper Technologies, Munich, Germany). Then, 100 μL of 20 μM transgelin solutions and 100

µL of 60 µM NT647-NHS fluorophore (NanoTemper Technologies) were mixed and incubated at room temperature for 30 min. Monolith NT.115 instrument was used to examine the interaction of NT647-transgelin and Deg-AZM. The mixtures were loaded in standard-treated capillaries and detected through MST at the powers of 20% and 80% and light-emitting diode intensity of 30%.

Negative staining electron microscopy. The copper mesh of the carbon film was first subjected to hydrophilic treatment. Next, 3 µL of the sample solution (actin, actin/transgelin, and actin/transgelin/Deg-AZM) was placed on the carbon film and then held for 1 min. Excess sample liquid was removed from the copper edge. A drop of phosphotungstic acid dye was added, incubated for 1 min, and air-dried at room temperature. Extra dye was removed as well. The samples were ready for observation through cryogenic electron microscopy (FEI Talos F200C, USA).

Preparation of transgelin-1 and actin. The BamHI restriction site of primers was added to the upstream of the start codon, and the XhoI restriction site was added to the downstream of the stop codon. PCR analysis was performed with the final reaction volume of 50 µL. Afterward, 0.5 µM primers, 1 µL of DNA polymerase, and 1 µL of cDNA were added. The PCR program was run for 5 min at 95 °C, followed by 30 cycles for 30 s at 95 °C and 30 s at 62 °C. A single PCR product was determined on the basis of the melting curve. Inserts were digested with BamHI and XhoI restriction enzymes and then purified. The digested inserts were ligated into the pET28a vector and verified by DNA sequencing. The plasmid coding for 6 His-tagged transgelin was transformed into BL21 (DE3) *E. coli* cells for protein expression. *E. coli* cells were cultivated at 37 °C in 800 mL of Luria–Bertani medium until the D600 of the culture reached 0.7. Then, IPTG was added at the final concentration of 1 mM, and the mixture was agitated overnight at 16 °C. Cell particles were resuspended in buffer A (20 mM Tris-HCl, 500 mM NaCl, and 5% glycerin; pH 8.0) and then lysed. The lysate was centrifuged at 10,000 rpm at 4 °C for 30 min. The Ni-NTA column was washed with 1 M imidazole and loaded with the supernatant. Buffer B (20 mM Tris/HCl, 500 mM NaCl, 5% glycerin, and 20 mM imidazole; pH 8.0) was used to minimize contamination by other proteins. Protein was eluted in buffer C (20 mM Tris/HCl, 500 mM NaCl, 5% glycerin,

and 200 mM imidazole; pH 8.0). The protein was concentrated to 0.5 mL by ultrafiltration with 10 kDa membranes and loaded onto an AKTA Explorer fast-performance liquid chromatography system with a Superdex 75 column (GE Healthcare, Sweden). The protein was collected and checked through SDS-PAGE (15%). Samples containing transgelin were concentrated to 15 mg/mL. Actin protein was purchased from Greenherbs Co., Ltd. (Beijing, China).

Detection of the antibacterial activity of Deg-AZM. The antibacterial activity of Deg-AZM was evaluated on the basis of its bacterial growth inhibition rate. In brief, test tube slants were inoculated with sterile loops in sterile water with glass beads and then agitated well for several minutes to allow spores to disperse evenly. Afterward, the solution was filtered to prepare a uniform spore suspension. A 0.5 mL aliquot of the mixed spore suspension was pipetted and injected into each Petri dish with a sterile pipette. The agar medium was melted, and 15–20 mL of the medium was poured into the dishes. Then, the medium and broth were mixed. Next, 5 µM Deg-AZM solution was decanted, and the prepared disc filter paper was immersed in the solution. Subsequently, the disc filter was removed, air-dried, and then placed at the center of the prepared plate culture medium. Then, it was covered with the Petri dish lid. The presence of the zone of inhibition around the round filter paper (Deg-AZM) was observed after 48–72 h of cultivation, and then the diameter of the zone of inhibition was calculated.

Effect of long-term Deg-AZM administration on intestinal microflora in mice. Experimental mice were divided into the control and Deg-AZM-treated groups. Deg-AZM (21.7 mg/kg, twice daily) was intragastrically administered to mice in the Deg-AZM-treated group for 4 weeks. Then, feces were collected from the colons of the control and Deg-AZM-treated mice in a sterile environment and frozen at −80 °C. Microflora sequencing assays were performed by Genergy Company (Shanghai, China).

Detection of Deg-AZM in fecal samples through mass spectrometry. Fecal samples were collected after the intragastric administration of AZM. Fecal samples incubated with AZM *in vitro* were also collected. Approximately 1 g of each fecal sample was homogenized in 1 mL of methanol:water (1:1, v/v), ultrasonicated for 10 min, and then

centrifuged at 15,000 g for 20 min. Then, 10 μL of the supernatant was injected into the HPLC system.

Samples were analyzed by using a HPLC–mass spectrometry system consisting of UltiMate 3000 × 2 Dual-Gradient HPLC system (Sunnyvale, CA, USA) and API 4000[+] triple quadrupole mass spectrometer (AB SCIEX, USA) equipped with an electrospray ionization source interface in positive-ion mode. The data acquisition software used was Analyst 1.6 (Toronto, Canada). The columns used were Acclaim ODS column (150 mm × 4.6 mm I.D., 5 μm particle size) (Thermo Fisher Scientific Inc., Waltham, MA, USA) and Venusil MP ODS guard column (10 mm × 4.6 mm I.D., 5 μm particle size) (Agela Technologies Wilmington, DE, USA). The mobile phase was a mixture of acetonitrile (A) and HPLC-grade water with 0.01% formic acid (B) at a flow rate of 1.0 mL/min. The HPLC gradient started at 85% mobile phase B and then was gradually reduced to 40% B within 6 min. Then, the same cycle was applied after the first cycle. The HPLC gradient process lasted for 13 min. MS/MS acquisition was operated in positive mode through multiple-reaction monitoring (MRM) with the following parameters: curtain gas, 30 psi; GAS1, 50 psi; GAS2, 60 psi; ion spray voltage, 5,500 V; ion source temperature, 500 °C; and CAD gas, 5 units. Three MRM channels were used to monitor Deg-AZM. Declustering potential, entrance potential, collision energy, and collision cell exit potential were analyzed individually under MRM acquisition, as shown in Table S6.

Detection of ATP, LDH, and ROS contents. HISMCs were treated with 20 μM Deg-AZM for 24 h. ATP, ROS, and LDH contents were then measured with ATP (S0026, Beyotime, Shanghai, China), ROS (S0033, Beyotime, Shanghai, China), and LDH cytotoxicity assay kits (C0016, Beyotime, Shanghai, China), respectively.

Location and distribution of Deg-AZM probes in cells under STORM. HISMCs were cultured at a density of 50%–60%, washed with PBS, fixed with 3% PFA and 0.1% glutaraldehyde for 10 min at room temperature, and treated with 0.1% NaBH4 for 10 min at room temperature to reduce the effect of unbound aldehyde on the cells because NaBH4 removes unbound aldehyde groups. The cells were washed thrice with PBS at room temperature every 5 min, treated with 5% BSA blocking antigen, and incubated

with 150 μL of primary antibody solution (Transgelin: ab14106, 1:100, Abcam; actin: 8H10D10, 1:50, CST, dissolved in blocking buffer) for 1 h at room temperature. The cells were washed with 1× PBS and incubated for 30 min with 150 μL of secondary antibody solution (Alexa Fluor® 488-conjugated goat anti-rabbit IgG and Alexa Fluor® 568-conjugated goat anti-mouse IgG dissolved in blocking buffer). The samples were protected from light at room temperature and well mixed. The cells were subsequently incubated with Deg-AZM probes for 1 h at room temperature, and washed thrice with 1× PBS. The cells were reacted with 200 μL of click reaction solution (Alexa Fluor™ 647 Azide) for 2 h at room temperature, washed thrice with 1× PBS, and imaged under a Ti-E inverted microscope (ORCA Flash4.0, sCOMS, Nikon, Japan).

Measurement of Deg-AZM tissue distribution. Two healthy females and one healthy male per one sampling time point group (4–6 weeks old) were used as the control group. Blank tissues, that is, the heart, liver, spleen, lung, kidney, stomach, duodenal, jejunum, ileum, cecum, colon, rectal tissue, and brain tissues, were collected from different healthy mice and stored at −80 °C until use.

Eighteen healthy mice were randomly divided into six groups. Each group comprised two female mice and one male mouse. Before the experiment, the mice were fed with normal diet for 3 days and fasted for 12 h before drug administration, but allowed to drink freely. Feeding was resumed 4 h after drug administration. Each group received 0.1 mL of 21.71 mg/mL Deg-AZM solutions through intragastric administration.

Then, 1 mL of blood samples was collected at 0.083 (5 min), 0.5 (30 min), 3, 6, 10, and 24 h from the eyeball (EP was stored in advance with heparin sodium). Mice were sacrificed and dissected after blood collection. Tissues from the heart, liver, spleen, lung, kidney, stomach, duodenum, jejunum, ileum, cecum, colon, rectum, brain, skeletal muscle, and bone marrow were obtained. Blood around the tissue was flushed with saline, and the gastrointestinal tissue was divided and cleaned. The Deg-AZM content of the tissues was detected through mass spectrometry.

Pharmacokinetics study of Deg-AZM. A single dose of Deg-AZM was administered intravenously and intragastrically before the collection of retrobulbar venous plexus blood. Fifteen healthy SD rats were randomly divided into three groups (n = 5) in

accordance with their BWs: oral low-dose group (10 mg/kg), oral medium-dose group (30 mg/kg), and intravenous injection group (5 mg/kg). Before the experiment, the mice in each group were fasted overnight with free access to water. Temporal venous plexus blood was collected prior to injection and at 2, 5, 15, 30, and 45 min and 1, 2, 4, 6, 8, 10, 12, and 24 h after injection through the tail vein. Blood was collected from the eyelid venous plexus before drug administration and at 5, 15, 30, and 45 min and 1, 2, 4, 6, 8, 10, 12, and 24 h after intragastric administration.

Electrophysiological experiment

The electrocardiogram (ECG) of the mice was obtained by using a multichannel electrophysiology instrument to observe whether DEG-AZM had a toxic effect on the heart of the mice. An ECG100C amplifier was used to acquire an ECG signal. The gain of the amplifier, the high-pass filter, and the low-pass filter were set at 2000, 0.05 Hz, and 35 Hz OFF, respectively. After the instrument was adjusted, the mice were anesthetized and connected with three electrodes. VIN+, VIN-, and GND were connected to the left lower limb, the right upper limb, and the right lower limb, respectively. After the original channel and acquisition parameters of the ECG signal were set, the signal was acquired.

Calcium clamping of HISMCs. A buffer solution was prepared by mixing10 mmol/L EGTA with a certain amount of Ca^{2+} in accordance with the Ca^{2+}–EGTA stability constant K. Cytoplasmic Ca^{2+} concentration can be fixed to a certain concentration by the influx of the buffer solution into the cytoplasm. This technique enables the identification of any agonist-initiated mechanism that may regulate cell contraction without changing cytoplasmic Ca^{2+} levels. Ca^{2+} concentration was set on the basis of the previously reported optimal Ca^{2+} concentration. Cells were divided into the control and Deg-AZM-treated groups (20 μM). Then, intercellular transgelin and actin were subjected to immunofluorescence staining and imaged using a confocal microscope (Nikon, Japan).

Gene set enrichment and Kyoto Encyclopedia of Genes and Genomes (KEGG) analysis. HISMCs (5×10^6 cells) were collected from Deg-AZM-treated (20 μM, 24h) and control groups. Cells were incubated with Trizol (1 mL) at room temperature for

15 min. Microarray gene expression profiling was performed by Genergy Company (Shanghai, China). R studio analysis tool was used to detect differentially expressed genes (DEGs) with $|logFC| \geq 2$ as the cut-off criterion. The differentially expressed genes (DEGs) in the Deg-AZM-treated and control groups were enriched through GO analysis by using the GSEA software (version 3.0, Gene ontology gene sets: c5.all.v6.1.symbols.gmt). DEGs were subjected to KEGG analysis by using the KEGG Automatic Annotation Server (http://www.genome.jp/kaas-bin/kaas_main?prog=GHOSTX&way=s).

Statistical analysis. Statistical analyses were performed by using Prism software (GraphPad Software). Data from biological triplicate experiments were presented with error bar as mean ± SD. Two-tailed unpaired Student's t-test was used for comparing two groups of data. One-ANOVA was used to compare multiple groups of data. $P < 0.05$ was considered statistically significant.

Supplementary Figures
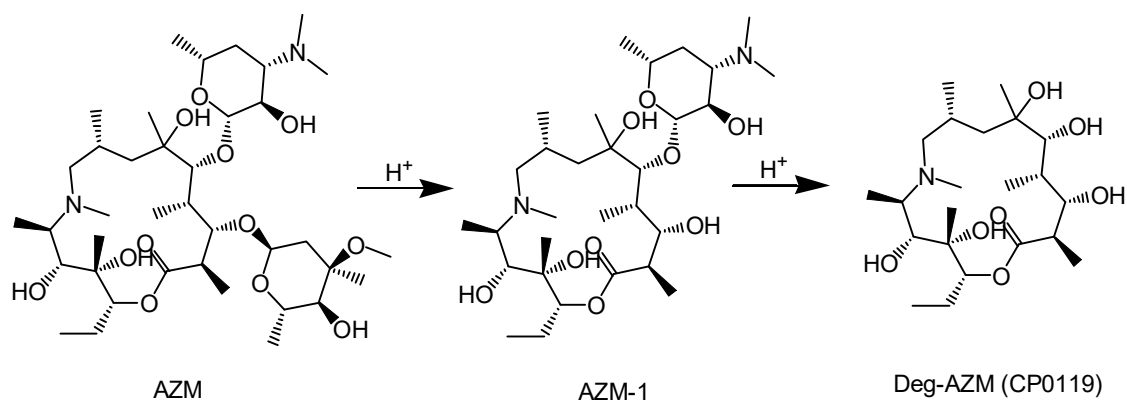
Figure S1. Synthesis step of AZM-1 and Deg-AZM, Related to Figure 3.
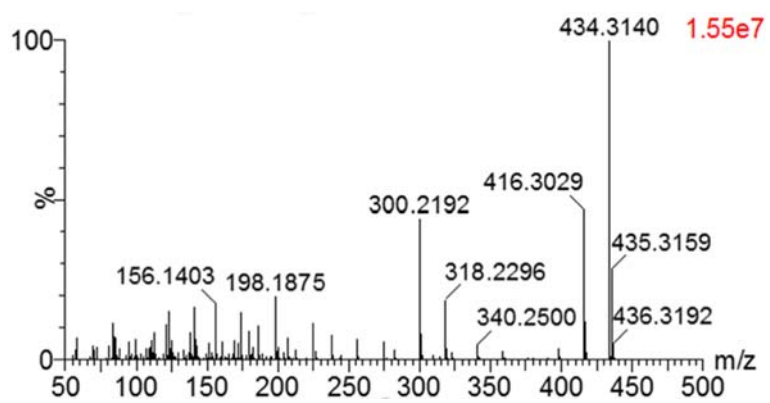
Figure S2. High resolution data of Deg-AZM, Related to Figure 3.
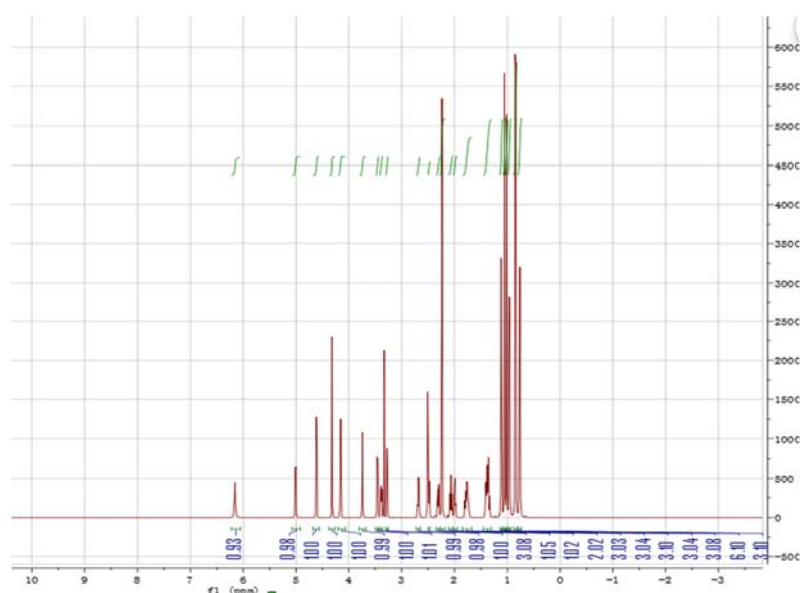
Figure S3. Nuclear magnetic hydrogen spectrum characterization result of Deg-AZM, Related to Figure 3. ^{1}H NMR (400 MHz, DMSO-d6) δ 6.13 (s, 1H), 4.98 (dd, J = 11.0, 2.4 Hz, 1H), 4.58 (d, J = 5.7 Hz, 1H), 4.29 (s, 1H), 4.13 (d, J = 8.4 Hz, 1H), 3.72 (d, J = 4.7 Hz, 1H), 3.44 (dd, J = 8.4, 1.3 Hz, 1H), 3.38– 3.33 (m, 1H), 3.25 (d, J = 4.7 Hz, 1H), 2.66 (d, J = 6.9 Hz, 1H), 2.45 (d, J = 6.8 Hz, 1H), 2.28 (dd, J = 12.4, 3.4 Hz, 1H), 2.21 (s, 3H), 2.04 (t, J = 12.0 Hz, 1H), 1.97 (q, J = 7.1 Hz, 1H), 1.82– 1.66(m, J = 15.5, 7.9, 3.9 Hz, 2H), 1.43 – 1.29 (m, 3H), 1.09 (d, J = 6.7 Hz, 3H), 1.03 (s, 3H), 0.99 (s, 3H), 0.94 (d, J = 6.7 Hz, 3H), 0.82 (d, J = 7.0 Hz, 6H), 0.74 (t, J = 7.3 Hz, 3H).
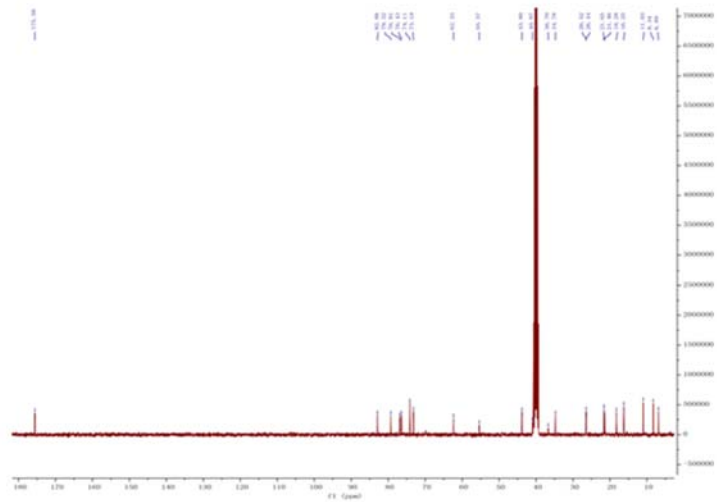
Figure S4. Carbon spectrum characterization result of Deg-AZM, Related to Figure 3.
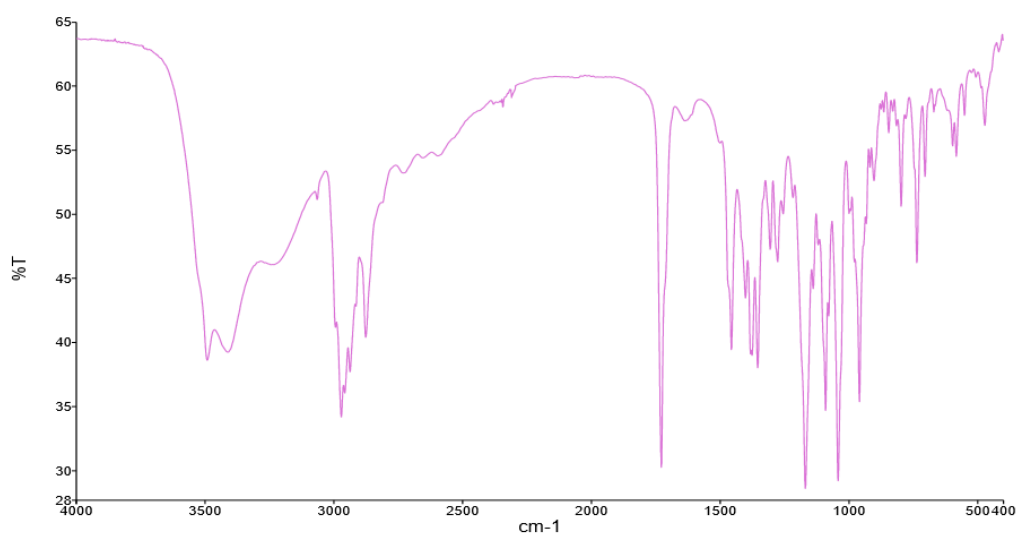
Figure S5. Infrared characterization result of Deg-AZM, Related to Figure 3. υmax（KBr）：

3493, 3413,2972,2958,2938,1728,1276,1254,1216,1168,1138 cm^{-1}.
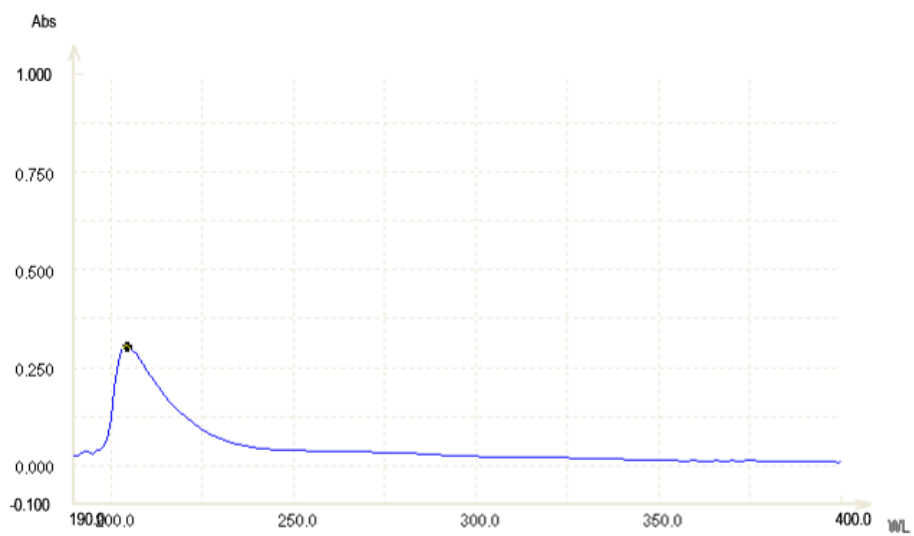
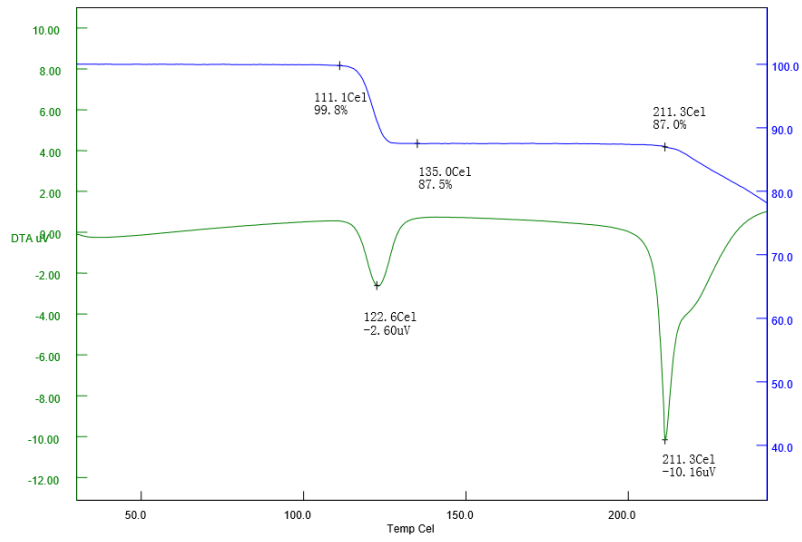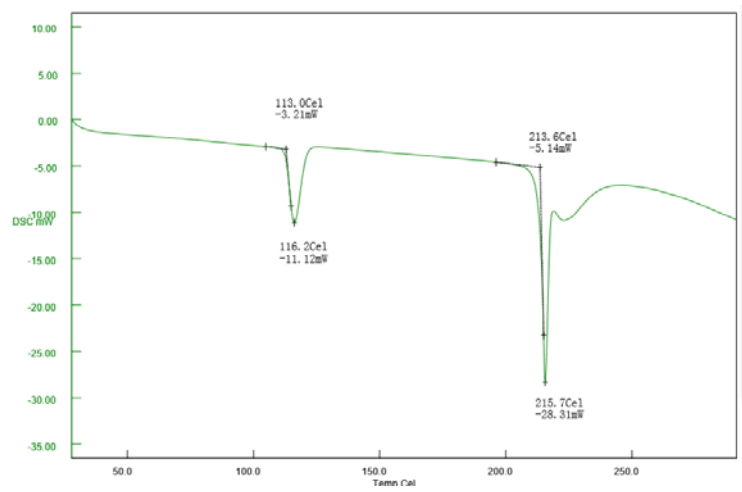Figure S6. UV scanning result of Deg-AZM, Related to Figure 3.

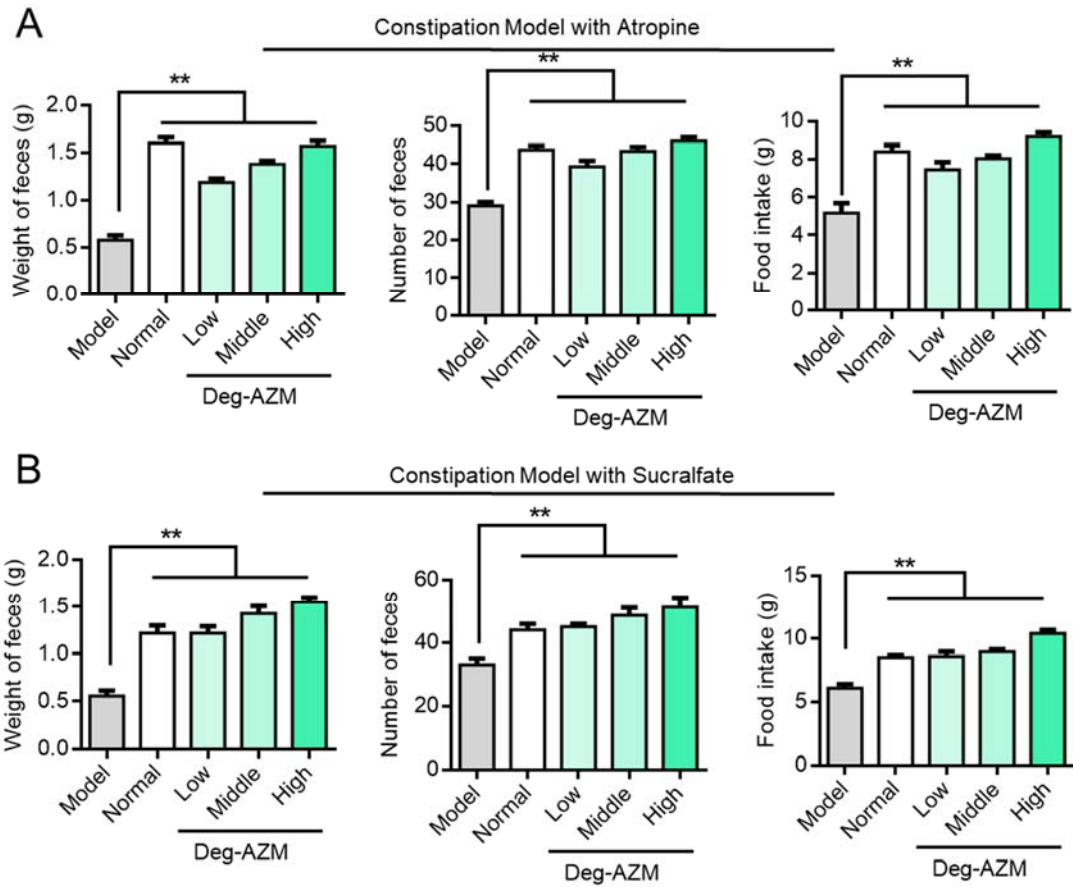Figure S7. DSC analysis result of Deg-AZM, Related to Figure 3.

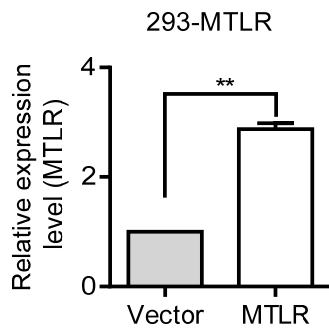**Figure S8.** The weight of feces, number of feces and animal food intake after Deg-AZM administrated, Related to Figure 3.

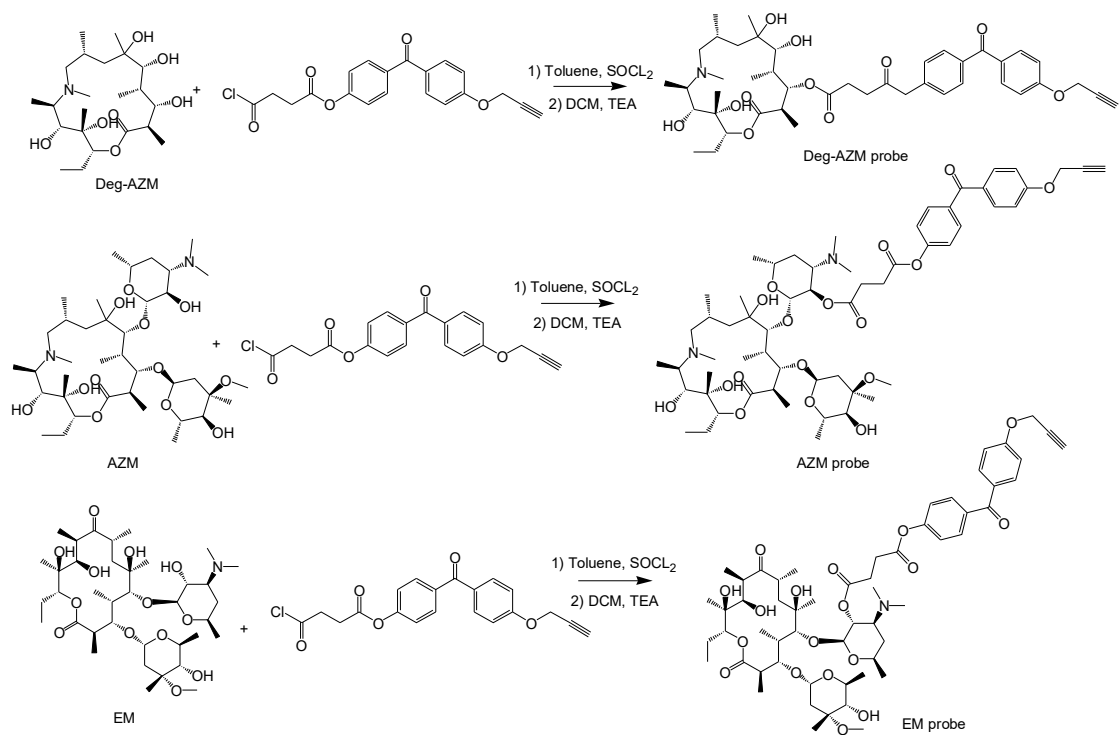Figure S9. Motilin receptor (MTLR) model in stable 293 cell lines, Related to Figure 4.

Figure S10. Synthesis step of Deg-AZM probe, AZM probe and EM probe, Related to Figure 4.
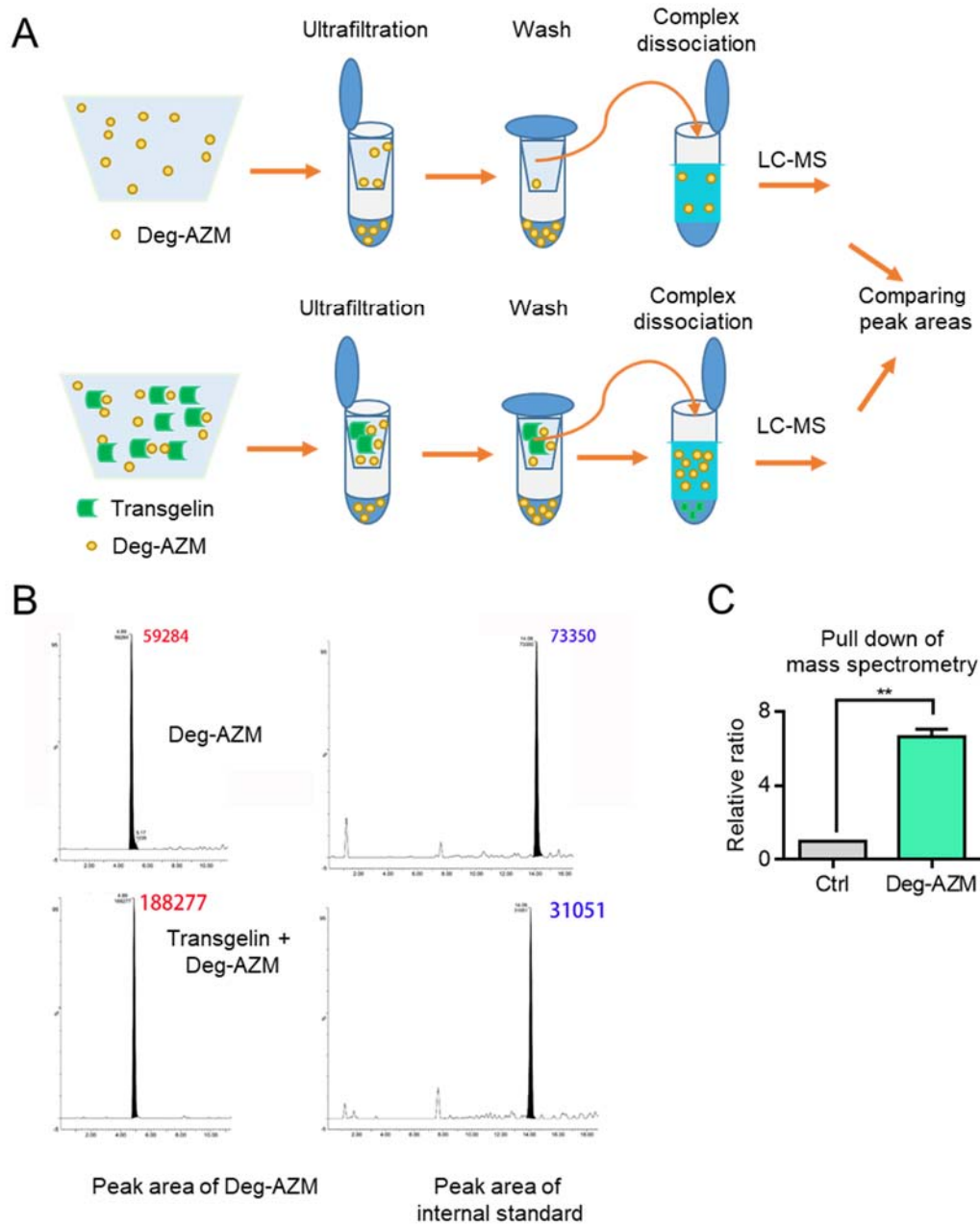
Figure S11. Schematic of indirect approaches for detection of Deg-AZM bind to transgelin,
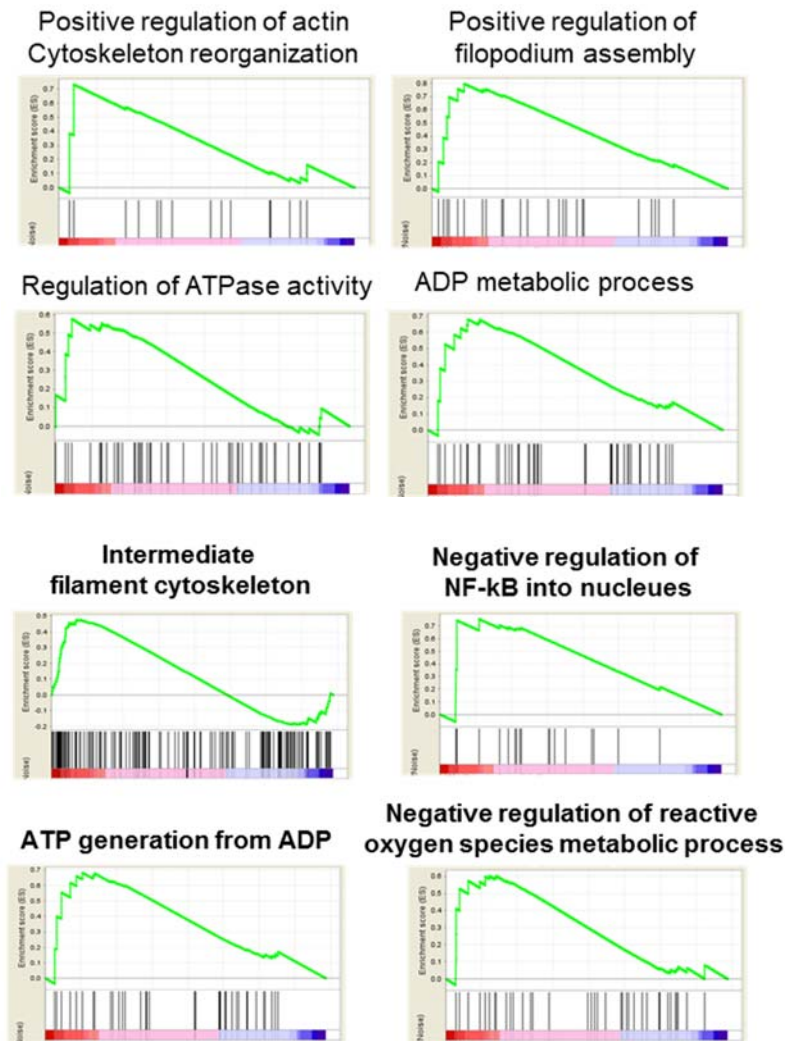
Related to Figure 5.

Figure S12. Gene Oncology analysis of differentially expressed genes in control and Deg-AZM
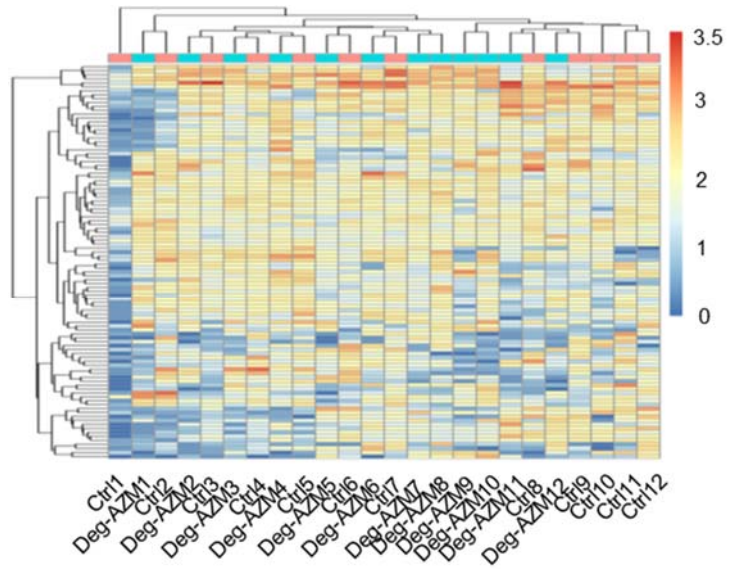
treated group, Related to Figure 6.

Figure S13. Cluster analysis of intestinal flora sequencing results in ctrl group and Deg-AZM treated group, Related to Figure 8.
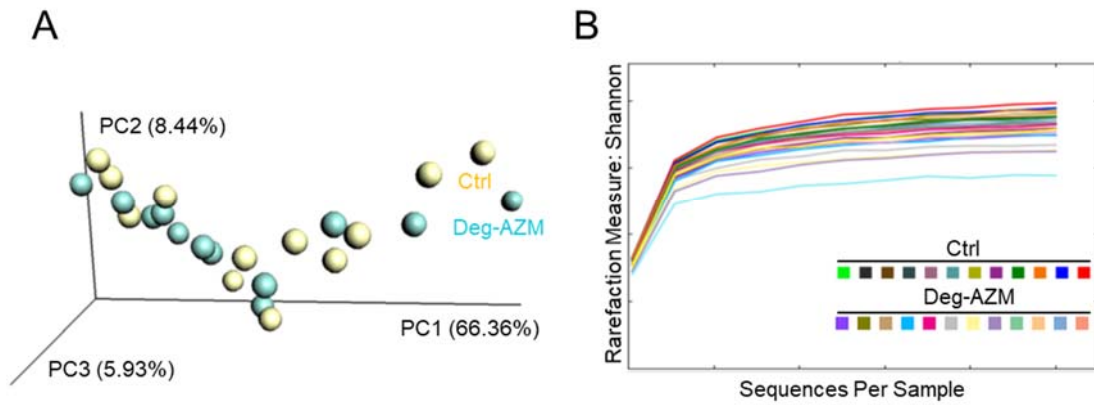
Figure S14. (A) Principal component analysis of control and Deg-AZM treated group. (B) Shannon analysis of control and Deg-AZM treated group. Results showed no significant difference in the 16s rRNA data between the control and Deg-AZM-treated groups, Related to Figure 4.
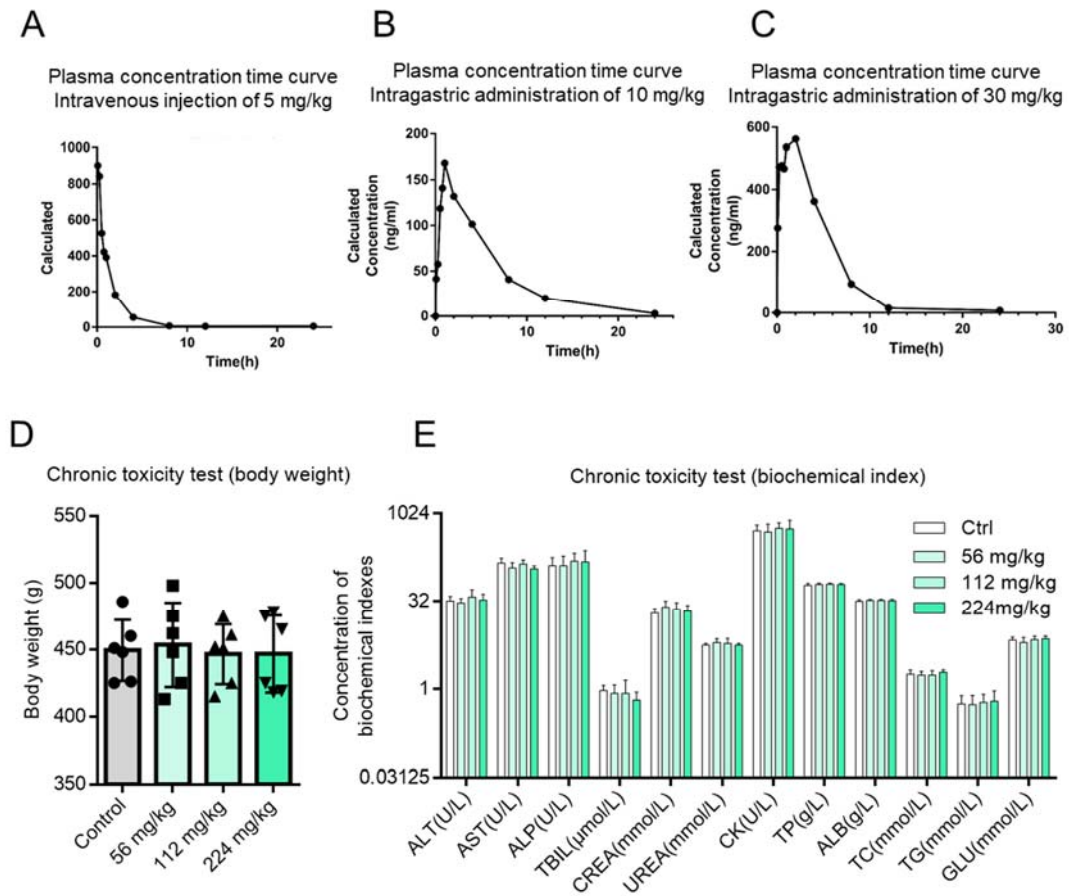
Figure S15. (A) Average blood drug concentration–time curve of rat intravenous injection of 5 mg/kg Deg-AZM. (B) Average blood drug concentration–time curve of rat intragastric administration of 10 mg/kg Deg-AZM. (C) Average blood drug concentration–time curve of rat intragastric administration of 30 mg/kg Deg-AZM. (D) Long-term toxicity of Deg-AZM in rats. (E) Detection of biochemical indicators in long-term toxicity test of DEG-AZM, Related to Figure 8.
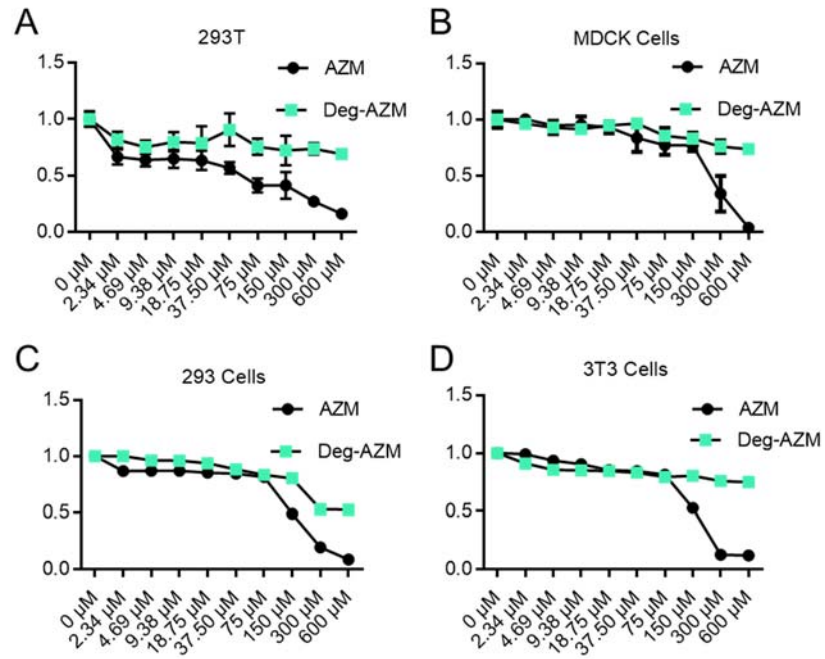
Figure S16. Cytotoxicity assay of Deg-AZM, Related to Figure 8.

Supplementary Tables

Table S1. Composition of control diet, Related to Figure 3.

Composition	Content
Protein,%	20
Carbohydrate,%	64
Fat,%	16
Casein	800
Cystine	12
Maltodextrin	528
Sucrose	400
Soybean oil	630
Vitamin mixture	40

Table S2. Potential Deg-AZM targets by use of affinity-based probe, Related to Figure 5.

Accession	Entry	mW (Da)	pI	PLGS Score	Peptides	Coverage (%)
P37804	TAGLN	22561	9.223	544.051	17	32.338
B1ASE2	B1ASE2	15872	4.923	223.226	3	23.913
Q8BGZ7	K2C75	59703	8.461	149.517	5	5.082
Q8BN83	Q8BN83	11971	9.486	131.129	1	10.092
Q91Z98	CHIL4	44946	5.751	46.242	1	3.483

Table S4. Molecular dynamics simulation results of Deg-AZM, EM and AZM binding with transgelin, Related to Figure 4.

Compounds	Deg-AZM	EM	AZM
Docking score	-3.548	No pose	-2.975
H_bonds	2		2
Binding energy	-123.55		-100.81
ELE	-827.16		-683.02
VDW	-144.54		-144.37
INT	0.00		-0.00

GAS	-971.70	-827.39
PBSUR	-15.67	-16.06
PBCAL	832.16	708.79
PBSOL	816.49	692.74
PBELE	5.01	25.77
PBTOT	-155.21	-134.65
GBSUR	-15.67	-16.06
GB	863.82	742.64
GBSOL	848.15	726.58
GBELE	36.66	59.62
GBTOT	-123.55	-100.81

Table S5. Inhibition ratio of the Deg-AZM to hERG current and IC_{50} results, Related to Figure 8.

Compound	hERG current suppression ratio (%)					n	IC_{50}
	0.3 μM	1 μM	3 μM	10 μM	30 μM		
Deg-AZM	5.05% ± 3.68%	3.88% ± 0.99%	4.54% ± 2.46%	7.89% ± 2.76%	9.95% ± 1.73%	3	>30 μM

Table S6. MS/MS parameters for analyses Deg-AZM, Related to Figure 1.

Analytes	Q1 mass (m/z)	Q3 mass (m/z)	DP (V)	EP (V)	CE (V)	CXP (V)
Deg-AZM	434.3	58.1	90	10	80	10
		123.2	90	10	55	7
		300.2	90	10	39	18

References

Bazanova, S.V., Klement'Ev, F.V., and Kiseleva, K.I. (1954). [Comparative effects of atropin, lidol and thiphen in therapy of diskinetic constipation]. Sov Med *18*, 29-31.